

CRITICAL REVIEW

[View Article Online](#)  
[View Journal](#) | [View Issue](#)



Cite this: *RSC Sustainability*, 2024, **2**, 265

## Graphitic carbon nitride ( $\text{g-C}_3\text{N}_4$ ) as an emerging photocatalyst for sustainable environmental applications: a comprehensive review

Dhavalkumar Bhanderi, Pratikkumar Lakhani and Chetan K. Modi \*

Graphitic carbon nitride ( $\text{g-C}_3\text{N}_4$ ) stands as a prominent and sustainable photocatalyst, offering a transformative solution to pressing environmental and energy challenges. This review article provides a comprehensive examination of  $\text{g-C}_3\text{N}_4$ , spanning its synthesis methods, structural properties, photocatalytic mechanisms, and diverse applications. By delving into various synthesis techniques and their respective merits, we reveal recent breakthroughs that underscore the material's growing significance. Unveiling the critical structural attributes governing photocatalytic performance, including bandgap, surface area, and porosity, we explore the impact of doping and modification on enhancing its capabilities. In elucidating the photocatalytic mechanisms, we showcase how  $\text{g-C}_3\text{N}_4$  facilitates crucial processes like water splitting, pollutant degradation, and solar-driven carbon dioxide reduction, emphasizing its unique selectivity and efficiency. Through concrete examples and case studies, we highlight its versatility in applications ranging from water purification to hydrogen production and air quality enhancement, underscoring the environmental and economic benefits that come with its adoption. Challenges such as quantum efficiency and charge carrier recombination are addressed, alongside a forward-looking perspective on emerging trends and innovations. Ultimately, this review positions  $\text{g-C}_3\text{N}_4$  as a sustainable game-changer in the realm of environmental and energy technologies, offering a promising path towards a more sustainable future.

Received 23rd October 2023

Accepted 4th December 2023

DOI: 10.1039/d3su00382e

[rsc.li/rscsus](http://rsc.li/rscsus)

### Sustainability spotlight

Graphitic carbon nitride ( $\text{g-C}_3\text{N}_4$ ) is emerging as a promising catalyst in the realm of sustainable environmental applications. Its unique properties, including efficient light absorption and electron-hole pair generation, make it a key player in addressing pressing environmental challenges. By utilizing  $\text{g-C}_3\text{N}_4$  as a photocatalyst, we are taking a significant step towards a greener and cleaner future. This sustainable innovation paves the way for eco-friendly solutions in wastewater treatment, air purification, and renewable energy production, marking a brighter path towards a more sustainable planet.

## 1. Introduction

In an era characterized by escalating environmental challenges and the unrelenting pursuit of sustainable solutions, photocatalysis has emerged as a transformative technology with the potential to revolutionize our approach to pressing global issues.<sup>1–3</sup> The ability to harness sunlight and convert it into a powerful driving force for a myriad of chemical reactions holds the promise of addressing some of the most urgent concerns facing society today.<sup>4–7</sup> Among the plethora of photocatalytic materials, graphitic carbon nitride ( $\text{g-C}_3\text{N}_4$ ) has risen to prominence, captivating the imagination of researchers and practitioners alike. Its unique combination of properties, including excellent stability, ease of synthesis, and a suitable

bandgap, positions it as an ideal candidate for sustainable applications, ranging from water purification and renewable energy production to air quality improvement and carbon management.<sup>8–12</sup>

The imperative for sustainable solutions in the face of mounting environmental challenges is undeniable. Water scarcity, pollution, and the depletion of fossil fuels have compelled humanity to explore novel technologies that mitigate these issues while minimizing environmental harm.<sup>13–16</sup> Photocatalysis, as an eco-friendly and energy-efficient process, has emerged as a ray of hope.<sup>17,18</sup> By exploiting semiconductor materials that can absorb solar radiation and catalyze chemical reactions, photocatalysis has the potential to transform pollutants into harmless byproducts, produce clean energy from sunlight, and address the daunting issue of global warming through carbon capture and utilization.<sup>19–22</sup>

The utilization of graphitic carbon nitride ( $\text{g-C}_3\text{N}_4$ ) as a photocatalyst has garnered substantial attention within the

Applied Chemistry Department, Faculty of Technology & Engineering, The Maharaja Sayajirao University of Baroda, Vadodara 390001, Gujarat, India. E-mail: [chetanmodi-appchem@msubaroda.ac.in](mailto:chetanmodi-appchem@msubaroda.ac.in); Tel: +91-265-2434188



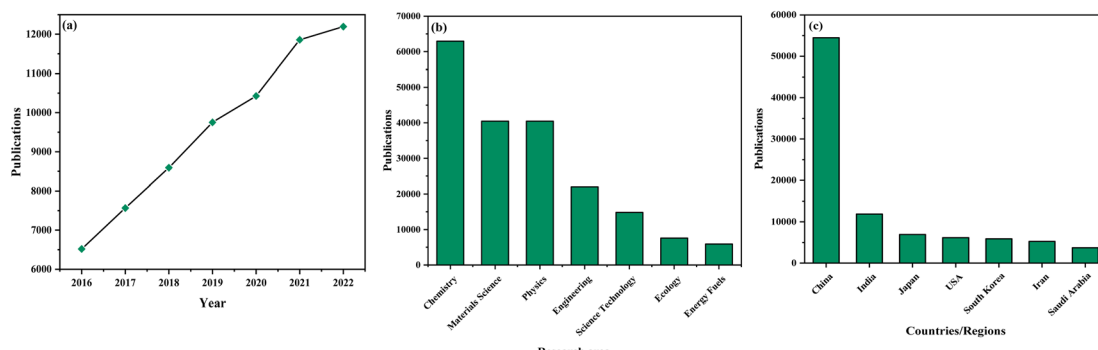


Fig. 1 Exploring the landscape of graphitic carbon nitride ( $g\text{-C}_3\text{N}_4$ ) as a photocatalyst: (a) number of publications in the past years, (b) distribution of the publications across scientific fields, and (c) worldwide distribution of publications (source: Web of Science).

scientific community, where a concerted effort is being made to decipher the distinctive qualities that render these catalysts truly exceptional. A thorough examination of literature resources accessible through prominent databases unveils a notable surge in publications pertaining to the application of graphitic carbon nitride ( $g\text{-C}_3\text{N}_4$ ) as a photocatalyst in recent times, indicative of a remarkable growth trajectory (as illustrated in Fig. 1(a)). This escalating trend emphatically underscores the escalating significance of graphitic carbon nitride ( $g\text{-C}_3\text{N}_4$ ) as a photocatalyst in the context of addressing intricate chemical transformations, sustainability-related challenges, and the formulation of environmentally friendly and more efficacious processes. Researchers are increasingly captivated by the extensive potential and the diverse array of applications offered by graphitic carbon nitride ( $g\text{-C}_3\text{N}_4$ ) as a photocatalyst, thereby reflecting the field's profound importance in shaping the future landscape of chemistry and sustainable technologies.<sup>23-28</sup>

Research in this field spans a broad spectrum of prominent scientific disciplines, with a central focus on areas including chemistry, materials science, physics, engineering, science technology, ecology, and energy fuels (as depicted in Fig. 1(b)). These research endeavors predominantly revolve around foundational and fundamental inquiries, representing a fundamental exploration into the core principles and mechanisms that govern the functionality of graphitic carbon nitride ( $g\text{-C}_3\text{N}_4$ ) as a photocatalyst. This interdisciplinary approach emphasizes the wide-ranging and profound implications associated with graphitic carbon nitride ( $g\text{-C}_3\text{N}_4$ ) as a photocatalyst, as it extends its influence into diverse scientific domains, ultimately accentuating its pivotal role in advancing our comprehension of chemical processes, sustainability practices, and the evolution of innovative technologies.<sup>29-34</sup>

The global landscape of publications in this field presents an intriguing picture, as depicted in Fig. 1(c). Notably, China emerges as the epicenter of active research on graphitic carbon nitride ( $g\text{-C}_3\text{N}_4$ ) as a photocatalyst, underlining the nation's significant contributions to the advancements in this particular domain. Following closely are India, Japan, and a host of other nations, all actively engaged in research pursuits pertaining to graphitic carbon nitride ( $g\text{-C}_3\text{N}_4$ ) as a photocatalyst. This

worldwide distribution underscores the widespread acknowledgment of the paramount importance of graphitic carbon nitride ( $g\text{-C}_3\text{N}_4$ ) as a photocatalyst across diverse regions on a global scale. Furthermore, it mirrors the collaborative and international character intrinsic to scientific research, with researchers hailing from various nations collectively striving to expand the frontiers of knowledge and devise sustainable solutions in the realm of photocatalysis.

While various photocatalysts have demonstrated promising capabilities, the distinctive properties of  $g\text{-C}_3\text{N}_4$  have thrust it into the limelight. Its structure, comprised of carbon and nitrogen atoms arranged in a two-dimensional conjugated framework, not only imparts exceptional chemical stability but also affords a favorable electronic band structure, making it well-suited for photochemical applications.<sup>35-38</sup> The synthesis of  $g\text{-C}_3\text{N}_4$  has been refined through diverse methods, offering researchers the flexibility to tailor its properties for specific applications. These methods encompass thermal polymerization, chemical vapor deposition, and solvothermal processes, among others, each with its own advantages and limitations.<sup>39-45</sup>

Intriguingly,  $g\text{-C}_3\text{N}_4$ 's remarkable photocatalytic performance extends beyond the realm of traditional semiconductor photocatalysts. Its capacity to generate electron–hole pairs upon exposure to light, facilitate charge separation, and participate in redox reactions has opened up new avenues for sustainable applications.<sup>46-48</sup> Whether it be the degradation of organic pollutants in water, the production of clean hydrogen fuel *via* water splitting, the removal of noxious gases from the atmosphere, or the conversion of carbon dioxide into value-added chemicals,  $g\text{-C}_3\text{N}_4$ 's versatility and efficiency have illuminated the path toward a more sustainable future.<sup>27,49-53</sup>

This comprehensive review endeavors to shed light on the multifaceted attributes of  $g\text{-C}_3\text{N}_4$  as a photocatalyst, exploring its synthesis techniques, structural properties, photocatalytic mechanisms, and diverse applications. It is our aspiration that by delving into the intricacies of  $g\text{-C}_3\text{N}_4$  photocatalysis, we can provide a roadmap for academic and industrial researchers to harness the immense potential of this material in advancing sustainability, catalyzing environmental stewardship, and paving the way for a cleaner, greener, and more sustainable world.



## 2. Synthesis methods

The synthesis of graphitic carbon nitride ( $\text{g-C}_3\text{N}_4$ ) has undergone significant development over the years, offering researchers a versatile toolkit to tailor its properties for specific photocatalytic applications. The following sections explore several key synthesis methods, each with its own advantages and limitations.

### 2.1 Thermal polymerization

One of the most widely employed methods for  $\text{g-C}_3\text{N}_4$  synthesis is thermal polymerization of low-cost precursors, such as melamine, urea, cyanamide, dicyanamide, thiourea, cyanuric acid *etc.* This process typically involves the heating of these precursors at moderate temperatures (around 500–600 °C) under inert gas atmospheres (Fig. 2). The thermal polymerization route generates a layered  $\text{g-C}_3\text{N}_4$  structure with a high surface area, making it suitable for various photocatalytic applications. The method's simplicity and cost-effectiveness have contributed to its popularity.<sup>54–56</sup>

### 2.2 Chemical vapor deposition (CVD)

CVD represents an alternative approach to  $\text{g-C}_3\text{N}_4$  synthesis, offering precise control over the material's thickness and morphology. In CVD, volatile precursors, such as cyanamide, are introduced into a high-temperature reactor, where they decompose and deposit as  $\text{g-C}_3\text{N}_4$  on substrates (shown in Fig. 3). This method allows for the growth of thin films and nanostructures, enabling applications in photovoltaics and optoelectronics. However, CVD may require more specialized equipment and is often associated with higher production costs.<sup>57–60</sup>

### 2.3 Solvothermal and hydrothermal methods

Solvothermal and hydrothermal routes involve the reaction of precursors in high-pressure, high-temperature aqueous or organic solvents (Fig. 4). These methods offer control over the morphology and structure of  $\text{g-C}_3\text{N}_4$  by adjusting reaction conditions. Solvent selection plays a crucial role in influencing the final product's properties. Hydrothermal synthesis is particularly effective in producing hierarchical  $\text{g-C}_3\text{N}_4$

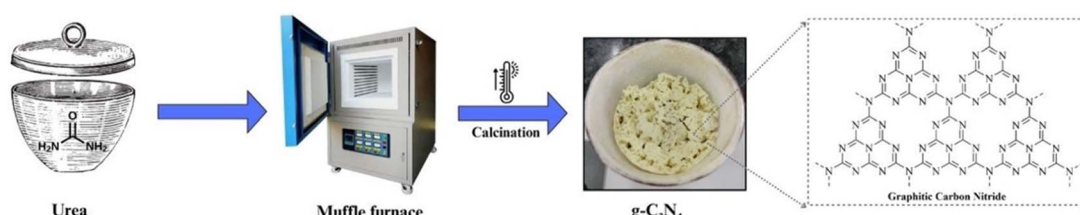


Fig. 2 Synthesis of  $\text{g-C}_3\text{N}_4$  via thermal polymerization method.

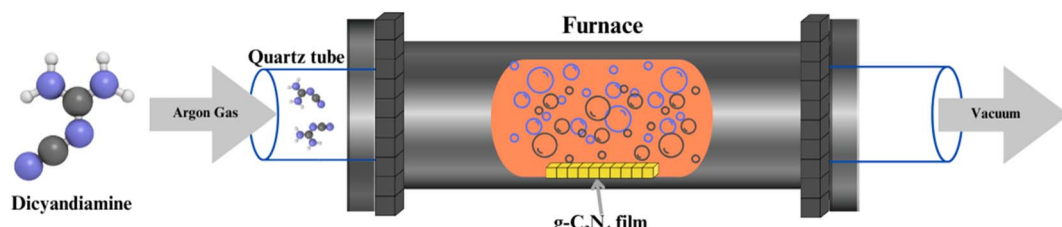


Fig. 3 Synthesis of  $\text{g-C}_3\text{N}_4$  via CVD method.

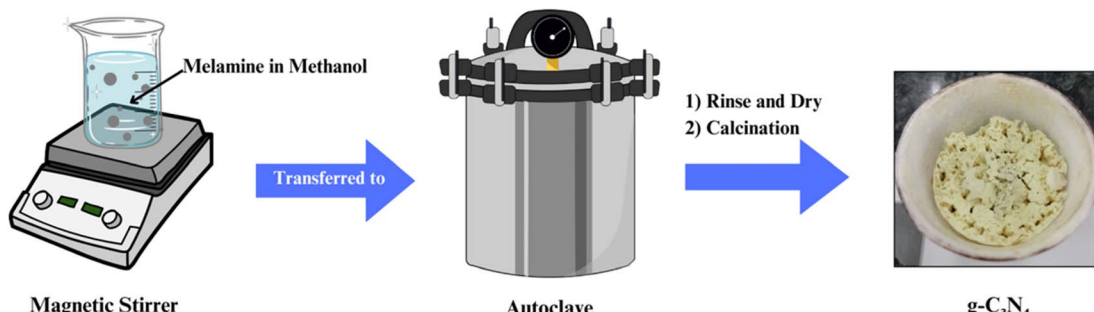


Fig. 4 Hydrothermal synthesis of  $\text{g-C}_3\text{N}_4$  particles.



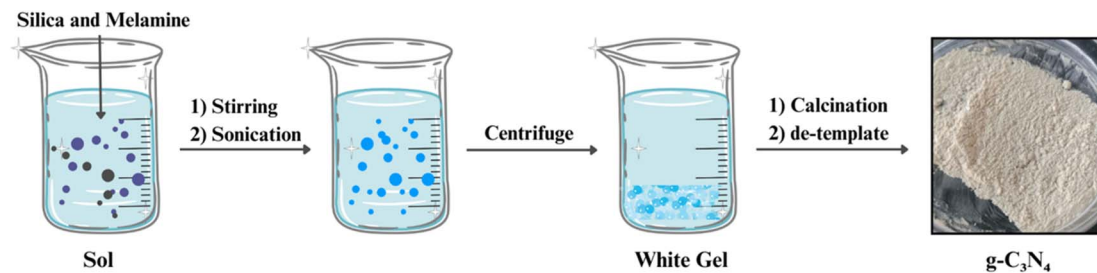


Fig. 5 Template-assisted synthesis of  $\text{g-C}_3\text{N}_4$  particles.

structures with enhanced photocatalytic activity. These methods are advantageous for tailoring  $\text{g-C}_3\text{N}_4$  for specific applications and have gained prominence in recent years.<sup>61–65</sup>

#### 2.4 Template-assisted synthesis

Template-assisted synthesis involves the use of templates, such as mesoporous silica or carbonaceous materials, to guide the formation of  $\text{g-C}_3\text{N}_4$  with specific structures (Fig. 5). By using templates with desired pore sizes and shapes, researchers can control the surface area and porosity of  $\text{g-C}_3\text{N}_4$ , which are critical factors affecting its photocatalytic performance. This approach enables the creation of  $\text{g-C}_3\text{N}_4$  materials with finely tuned properties for applications like pollutant removal and solar energy conversion.<sup>66–70</sup>

#### 2.5 Doping and co-doping strategies

To further enhance the photocatalytic activity of  $\text{g-C}_3\text{N}_4$ , doping and co-doping with other elements, such as sulfur, boron, and metals, have been explored (as shown in Fig. 6). Doping introduces impurities into the  $\text{g-C}_3\text{N}_4$  lattice, modifying its electronic structure and creating additional active sites for photocatalytic reactions. Co-doping involves the simultaneous incorporation of two or more elements to achieve synergistic effects. These strategies play a pivotal role in improving  $\text{g-C}_3\text{N}_4$ 's efficiency and selectivity in various photocatalytic processes.<sup>71–75</sup>

The synthesis of graphitic carbon nitride ( $\text{g-C}_3\text{N}_4$ ) has advanced significantly, providing a diverse set of methods with distinct advantages and limitations. Thermal polymerization, involving low-cost precursors like melamine, offers simplicity and cost-effectiveness, resulting in a layered  $\text{g-C}_3\text{N}_4$  structure suitable for various applications. Chemical vapor deposition

(CVD) allows precise control over thickness and morphology but may entail higher production costs and specialized equipment. Solvothermal and hydrothermal methods, utilizing high-pressure and high-temperature conditions, provide morphology control and have gained popularity for tailoring  $\text{g-C}_3\text{N}_4$  properties. Template-assisted synthesis uses templates to guide specific structures, influencing surface area and porosity critical for photocatalytic performance. Doping and co-doping strategies enhance photocatalytic activity by modifying the electronic structure.

Comparing these methods reveals trade-offs in terms of cost, complexity, and yield. Thermal polymerization is cost-effective and straightforward but might lack precision. CVD offers control but at higher costs. Solvothermal and hydrothermal methods provide control over morphology but involve specialized conditions. Template-assisted synthesis allows tailored structures but might be more intricate. Doping strategies enhance performance but add complexity. The choice depends on desired properties and applications, influencing cost-effectiveness and efficiency.<sup>24</sup>

In summary, the choice of synthesis methods for  $\text{g-C}_3\text{N}_4$  is influenced by the desired properties and intended applications. Researchers and engineers can select from these diverse synthesis techniques to tailor  $\text{g-C}_3\text{N}_4$  materials that meet the specific demands of sustainable environmental applications, from water purification to renewable energy production.

### 3. Structural properties

Graphitic carbon nitride ( $\text{g-C}_3\text{N}_4$ ) exhibits a unique two-dimensional structure composed of carbon and nitrogen atoms, which imparts distinctive structural properties crucial

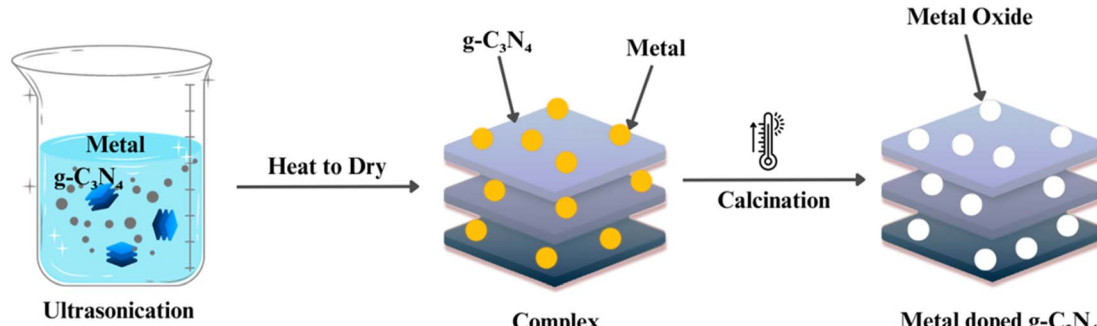


Fig. 6 Metal/metal oxide doped  $\text{g-C}_3\text{N}_4$  synthesis via doping strategies.



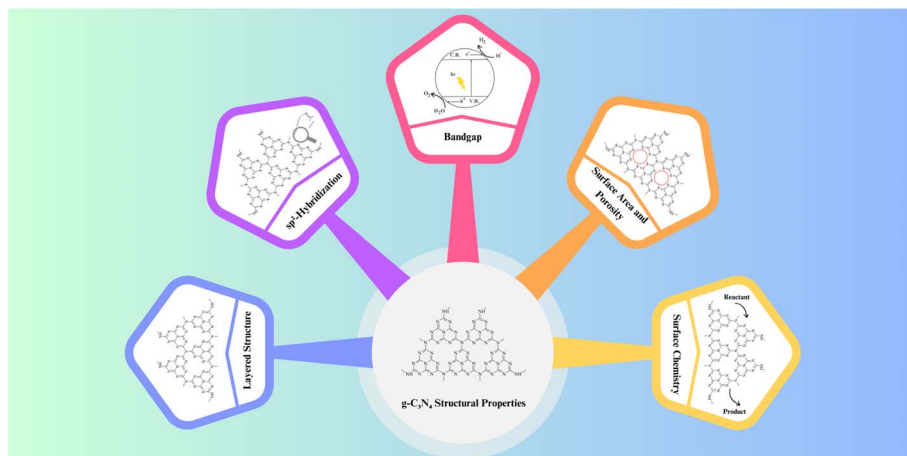


Fig. 7 Structural properties of pristine  $\text{g-C}_3\text{N}_4$ .

for its photocatalytic performance.<sup>76</sup> Understanding these properties is essential for tailoring  $\text{g-C}_3\text{N}_4$  materials to specific applications and optimizing their efficiency. The key structural attributes are provided in Fig. 7.

### 3.1 Layered structure

At its core,  $\text{g-C}_3\text{N}_4$  consists of stacked layers of carbon and nitrogen atoms arranged in a planar, hexagonal lattice. This layered structure resembles that of graphite, giving rise to its name, "graphitic". Each layer is composed of tri-*s*-triazine ( $\text{C}_3\text{N}_3$ ) units, and the layers are held together by weak van der Waals forces. This layered configuration provides a large surface area for potential reactant adsorption and photocatalytic reactions, making  $\text{g-C}_3\text{N}_4$  an attractive material for various applications.<sup>36</sup>

### 3.2 $\text{sp}^2$ -hybridization

The carbon atoms within the  $\text{g-C}_3\text{N}_4$  lattice adopt  $\text{sp}^2$ -hybridization, resulting in trigonal planar geometry. This  $\text{sp}^2$ -hybridized carbon configuration is responsible for the formation of delocalized  $\pi$ -bonds, contributing to the material's excellent electrical conductivity and optical properties. This electron-rich network facilitates charge carrier mobility and separation, which are essential for efficient photocatalysis.<sup>34</sup>

### 3.3 Bandgap

The electronic band structure of  $\text{g-C}_3\text{N}_4$  plays a pivotal role in its photocatalytic activity. It exhibits a moderate bandgap typically around 2.7 to 2.8 eV, making it responsive to visible light. Photons with energy equal to or greater than the bandgap can excite electrons from the valence band to the conduction band, initiating the photocatalytic process. The bandgap value allows  $\text{g-C}_3\text{N}_4$  to harness a substantial portion of the solar spectrum, rendering it effective for solar-driven applications.<sup>31</sup>

### 3.4 Surface area and porosity

The layer-by-layer structure of  $\text{g-C}_3\text{N}_4$  results in a high surface area, providing ample sites for reactant adsorption and subsequent photocatalytic reactions. The interlayer spacing between

$\text{g-C}_3\text{N}_4$  layers can be tuned to create mesopores and micropores, further enhancing its surface area and porosity. These structural features facilitate efficient mass transport and reactant accessibility, promoting photocatalytic efficiency.<sup>7</sup>

### 3.5 Surface chemistry

The surface of  $\text{g-C}_3\text{N}_4$  can be modified through functionalization, which introduces various functional groups such as amino, hydroxyl, and carboxyl groups. These modifications can influence the material's surface charge, hydrophilicity, and chemical reactivity, thus tailoring its suitability for specific photocatalytic applications. Surface functionalization also enables the attachment of co-catalysts, enhancing charge separation and overall photocatalytic performance.<sup>31</sup>

Moving to structural properties,  $\text{g-C}_3\text{N}_4$ 's layered structure,  $\text{sp}^2$ -hybridization, moderate bandgap, high surface area, and porosity are key features. The layered structure provides a large surface area for reactions, while  $\text{sp}^2$ -hybridization contributes to electrical conductivity. The moderate bandgap (2.7–2.8 eV) enables responsiveness to visible light, crucial for solar-driven applications. High surface area and porosity, achieved through the layer-by-layer structure and tuned interlayer spacing, facilitate efficient mass transport and reactant accessibility. Surface chemistry, modified through functionalization, further tailors properties for specific applications.<sup>24</sup> Understanding these structural properties allows researchers to design and engineer  $\text{g-C}_3\text{N}_4$  materials with optimized characteristics for diverse photocatalytic applications. By tailoring the layer spacing, bandgap, and surface chemistry,  $\text{g-C}_3\text{N}_4$  can be fine-tuned to address specific environmental and energy challenges, contributing to a sustainable and cleaner future.

## 4. Photocatalytic mechanism

The remarkable photocatalytic activity of graphitic carbon nitride ( $\text{g-C}_3\text{N}_4$ ) stems from its unique structural and electronic properties, which enable it to initiate and accelerate photochemical reactions under illumination. Understanding the underlying photocatalytic mechanisms is pivotal for harnessing



the full potential of  $\text{g-C}_3\text{N}_4$  in sustainable environmental and energy applications. The primary steps involved in the photocatalytic mechanism of  $\text{g-C}_3\text{N}_4$  are depicted in Scheme 1.<sup>77-79</sup>

The modification of  $\text{g-C}_3\text{N}_4$  is important for photocatalytic applications. The interface formed can reduce the recombination of photoinduced charge and improve the absorptivity of visible light. Meanwhile, the high redox ability of electrons and holes is maintained. Therefore, design and synthesis of different types of  $\text{g-C}_3\text{N}_4$ -based heterojunction photocatalysts has important research value for achieving efficient photodegradation of pollutants and improving the increasingly serious environmental pollution. In recent years, photocatalysts for type II-heterojunctions,  $\text{g-C}_3\text{N}_4$ -based p-n heterojunctions and Z-scheme heterojunctions have been developed rapidly and have shown great potential advantages in various photocatalytic systems. By constructing different types of heterostructures, the photocatalytic performance of  $\text{g-C}_3\text{N}_4$  has been greatly improved.<sup>80</sup>

#### 4.1 Light absorption and electron–hole generation

When  $\text{g-C}_3\text{N}_4$  is exposed to photons with energy equal to or greater than its bandgap (typically around 2.7 to 2.8 eV), electrons in the valence band are excited to the conduction band,

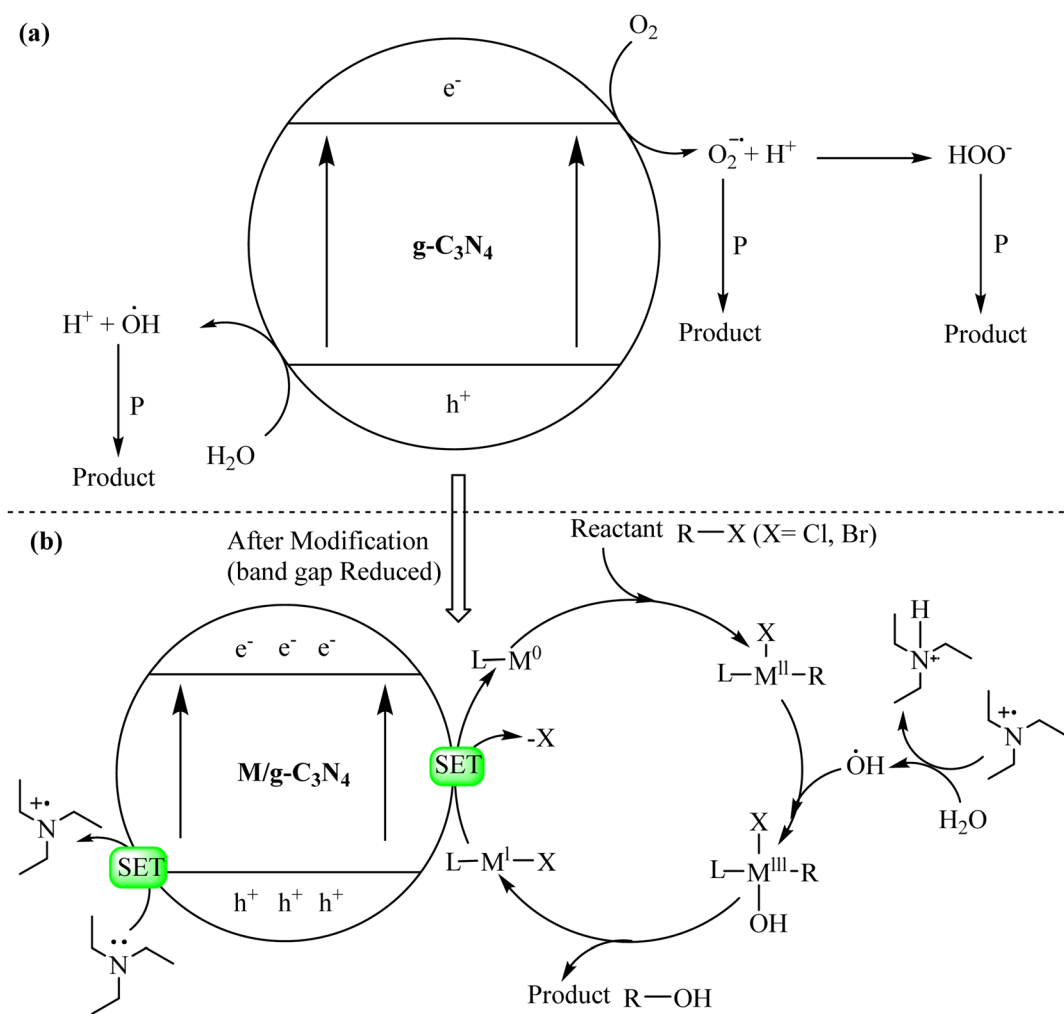
creating electron–hole pairs. This initial step is the foundation of photocatalysis, as it generates highly reactive species that can drive subsequent reactions.

#### 4.2 Charge separation

Once electron–hole pairs are generated, the electrons and holes become mobile within the  $\text{g-C}_3\text{N}_4$  lattice. Efficient charge separation is crucial to prevent recombination of electrons and holes, which would diminish photocatalytic efficiency. The unique layered structure of  $\text{g-C}_3\text{N}_4$ , with its  $\text{sp}^2$ -hybridized carbon atoms, facilitates rapid charge separation, allowing electrons to move freely through the lattice.

#### 4.3 Redox reactions

The separated electrons and holes are poised to participate in redox reactions on the  $\text{g-C}_3\text{N}_4$  surface. Electrons in the conduction band are capable of reducing various species, while the holes in the valence band can oxidize substances. For instance, in the context of water purification, electrons can reduce water molecules to form hydroxyl radicals ( $\cdot\text{OH}$ ), which are highly reactive and effective at degrading organic pollutants.



Scheme 1 General mechanisms of (a)  $\text{g-C}_3\text{N}_4$  catalyzed reactions and (b) metal/ $\text{g-C}_3\text{N}_4$ -catalyzed visible light driven reactions.



#### 4.4 Reaction with adsorbates

Adsorption of target molecules or pollutants onto the g-C<sub>3</sub>N<sub>4</sub> surface is a critical prerequisite for their degradation. The large surface area and active sites provided by g-C<sub>3</sub>N<sub>4</sub> facilitate the adsorption of organic molecules, pollutants, or gases. Once adsorbed, these species can directly interact with the photo-generated electrons or holes, initiating degradation or transformation reactions.

#### 4.5 Oxygen activation (for oxygen-dependent reactions)

In reactions involving oxygen, g-C<sub>3</sub>N<sub>4</sub> can also activate molecular oxygen (O<sub>2</sub>) to form reactive oxygen species (ROS) like superoxide radicals (O<sup>2-</sup>) and singlet oxygen (<sup>1</sup>O<sub>2</sub>). These ROS further enhance the photocatalytic activity by participating in oxidation reactions and promoting the breakdown of organic pollutants.

#### 4.6 Surface states and co-catalysts

Surface states on g-C<sub>3</sub>N<sub>4</sub>, as well as co-catalysts like metal nanoparticles or semiconductors, can further enhance charge separation and facilitate specific reaction pathways. Co-catalysts, for example, can serve as electron sinks or sources, improving overall photocatalytic performance.

The specific photocatalytic mechanisms can vary depending on the target reaction and the environment in which g-C<sub>3</sub>N<sub>4</sub> is employed. Whether it's water splitting, pollutant degradation, or carbon dioxide reduction, g-C<sub>3</sub>N<sub>4</sub>'s ability to generate and effectively utilize electron–hole pairs makes it a versatile and efficient photocatalyst for a wide range of sustainable applications. By elucidating these fundamental photocatalytic mechanisms, researchers can design and optimize g-C<sub>3</sub>N<sub>4</sub>-based photocatalysts to achieve higher efficiency, selectivity, and stability, ultimately contributing to the advancement of sustainable technologies and environmental preservation.<sup>81-83</sup>

### 5. Applications

Graphitic carbon nitride (g-C<sub>3</sub>N<sub>4</sub>) has emerged as a versatile and eco-friendly photocatalyst with a remarkable ability to address pressing environmental and energy challenges. Its wide range of applications spans various domains, each contributing to the advancement of sustainability. Here, we delve into the diverse

and transformative applications of g-C<sub>3</sub>N<sub>4</sub>, elucidating its role in:

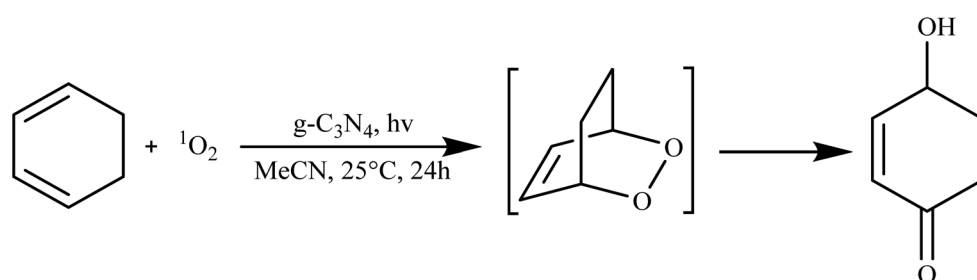
#### 5.1 Various organic transformations

g-C<sub>3</sub>N<sub>4</sub> has showcased its prowess in catalyzing various organic transformations, including the synthesis of organic chemicals, pharmaceuticals, and fine chemicals. Its unique surface chemistry and catalytic activity enable selective reactions, reducing the need for harsh reaction conditions and hazardous reagents. For instance, g-C<sub>3</sub>N<sub>4</sub> has been employed in the synthesis of diverse organic compounds, such as benzene derivatives, imines, and quinolines, showcasing its potential in green and sustainable chemistry.<sup>84</sup>

In their study, Quadrelli *et al.* found that when g-C<sub>3</sub>N<sub>4</sub> is oxidized, it exhibits excellent catalytic capabilities for generating singlet oxygen (<sup>1</sup>O<sub>2</sub>) under photochemical conditions. This particular form of graphitic carbon nitride, produced through the bulk and hard template pyrolysis of melamine, is considered a highly promising material for fostering environmentally-friendly chemical reactions. The oxidized g-C<sub>3</sub>N<sub>4</sub> catalyst, referred to as catalyst, demonstrated a range of performance levels, from satisfactory to outstanding, in the Diels–Alder cycloaddition reaction with *in situ* generated <sup>1</sup>O<sub>2</sub>, particularly in the case of 1,3-cyclohexadiene and with alkenes during ene reactions. Additionally, it displayed notable oxidative capabilities when interacting with aromatic olefins, as illustrated in Scheme 2.<sup>85</sup>

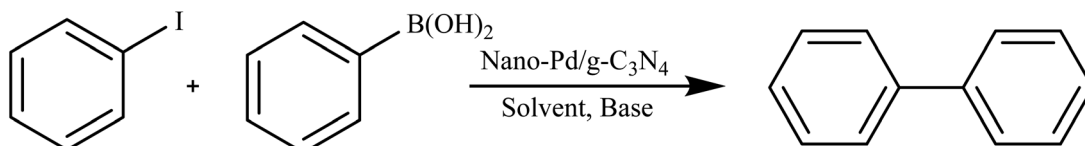
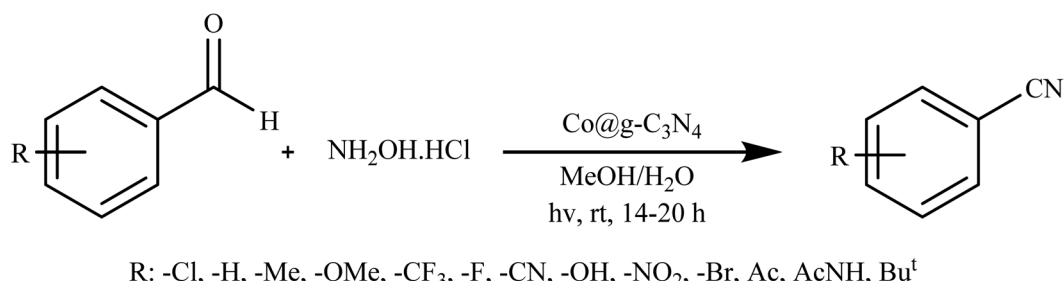
Sarkar *et al.* conducted a study on the utilization of a nano-Pd/gC<sub>3</sub>N<sub>4</sub> composite as a catalyst for the microwave-assisted Suzuki cross-coupling of various aryl halides with different arylboronic acids. The reactions took place in an aqueous medium under aerobic conditions. The catalyst proved to be exceptionally efficient, with impressive turnover frequencies (TOFs) of approximately 12 000 per hour across a range of substituted reactants. This work exemplifies an innovative and environmentally friendly approach to catalysis, combining the advantages of reusability, water as a solvent, and microwave irradiation as an alternative heating method, as depicted in Scheme 3.<sup>86</sup>

Rai *et al.* introduced an innovative and environmentally friendly process using visible light to efficiently convert aldehydes into nitriles. This method employs Co@g-C<sub>3</sub>N<sub>4</sub> as a photocatalyst in an aqueous environment, operating under normal ambient conditions, as illustrated in Scheme 4. Key attributes of



Scheme 2 Diels–Alder cycloaddition reaction via oxidized g-C<sub>3</sub>N<sub>4</sub> catalyst.



Scheme 3 Suzuki cross-coupling of various aryl halides via nano-Pd/g-C<sub>3</sub>N<sub>4</sub> composite.Scheme 4 Co@g-C<sub>3</sub>N<sub>4</sub> photocatalyst for conversion of aldehydes into nitriles.

this designed photocatalyst include its selectivity, stability, and reusability across multiple reactions. Its heterogeneous nature, combined with its effectiveness under ambient conditions, makes it a highly advantageous alternative for potential application in various industries.<sup>87</sup>

Yao and colleagues introduced an inventive technique for producing oxygen-doped carbon nitride material (OCN) through a hydrothermal-calcination method. The OCN material exhibited outstanding performance as a stable photocatalyst, displaying excellent efficiency and recyclability. This catalyst facilitated the creation of 3-arylquinoxalin-2(1*H*)-ones by catalytically breaking down aryl diazonium salts under blue light exposure, all accomplished without the utilization of metals or external additives, as illustrated in Scheme 5. This approach not only provides a novel, environmentally friendly, and easily recyclable pathway but also signifies a sustainable synthetic strategy for generating these valuable structural entities.<sup>88</sup>

The case study illustrates various catalytic systems (Table 1) such as oxidized g-C<sub>3</sub>N<sub>4</sub>, nano-Pd/g-C<sub>3</sub>N<sub>4</sub> composites, Co@g-C<sub>3</sub>N<sub>4</sub>, and oxygen-doped graphitic carbon nitride (OCN) which displayed remarkable performance in diverse organic transformation reactions. These innovative catalysts showcase assorted strengths, including high efficiency, recyclability, and environmental friendliness, providing a promising array of

options for sustainable and eco-friendly chemical synthesis across various industries.

In the realm of organic transformations, g-C<sub>3</sub>N<sub>4</sub> emerges as a formidable ally, ushering in a new era of sustainable chemistry. Its ability to facilitate selective reactions under mild conditions reduces the environmental footprint of chemical synthesis. From the creation of valuable pharmaceutical intermediates to the sustainable production of fine chemicals, g-C<sub>3</sub>N<sub>4</sub> showcases its versatility and eco-friendliness. As the world seeks greener and more sustainable pathways in the realm of chemical synthesis, g-C<sub>3</sub>N<sub>4</sub> stands as a beacon of hope, embodying the promise of harnessing solar-driven catalysis to meet the demands of a rapidly changing world, where sustainability and efficiency are paramount.

## 5.2 Hydrogen production through water splitting

The efficient utilization of solar energy to split water into hydrogen and oxygen holds the key to clean and renewable hydrogen production. g-C<sub>3</sub>N<sub>4</sub>'s bandgap aligns well with the solar spectrum, allowing it to harness sunlight for photocatalytic water splitting. By absorbing photons and generating electron-hole pairs, g-C<sub>3</sub>N<sub>4</sub> initiates the water splitting reaction, producing clean hydrogen fuel, a promising step toward a hydrogen-based economy.

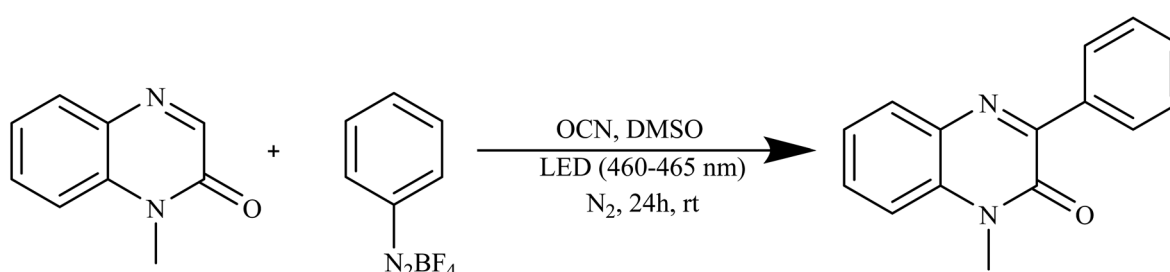
Scheme 5 Oxygen doped carbon nitride used as a catalyst for the synthesis of 3-arylquinoxalin-2(1*H*)-ones.

Table 1  $\text{g-C}_3\text{N}_4$ -based catalysts for various organic transformations

| Entry | Catalyst                              | Organic transformation                            | Yield (%) | Ref. |
|-------|---------------------------------------|---|-----------|------|
| 1     | $\text{g-C}_3\text{N}_4$              | Diels–Alder reaction                              | 55%       | 84   |
| 2     | $\text{Pd}@\text{g-C}_3\text{N}_4$    | Suzuki–Miyaura cross-coupling                     | 99%       | 85   |
| 3     | $\text{Co}@\text{g-C}_3\text{N}_4$    | Nitrile synthesis                                 | 92%       | 86   |
| 4     | Oxygen-doped $\text{g-C}_3\text{N}_4$ | Synthesis of 3-arylquinoxalin-2(1 <i>H</i> )-ones | 68%       | 87   |

Han *et al.* created  $\text{g-C}_3\text{N}_4$  composites with silver (Ag) using two methods: precipitation–calcination (DeCNexAg) and annealing (ZeCNexAg). These Ag-based composites exhibited enhanced photocatalytic activity under visible light. The best hydrogen production was achieved with DeCNexAg containing 5%  $\text{Ag}_2\text{CO}_3$ , producing 4.6 times more hydrogen than ZeCNex5% Ag. This enhanced performance was attributed to the presence of metallic Ag and additional active sites on the DeCNex5% Ag surface, aiding in charge separation and transfer. The study also highlighted the role of the local surface plasmon resonance (LSPR) effect and the close interaction between Ag and  $\text{g-C}_3\text{N}_4$  in improving hydrogen production through water splitting as shown in Fig. 8.<sup>89</sup>

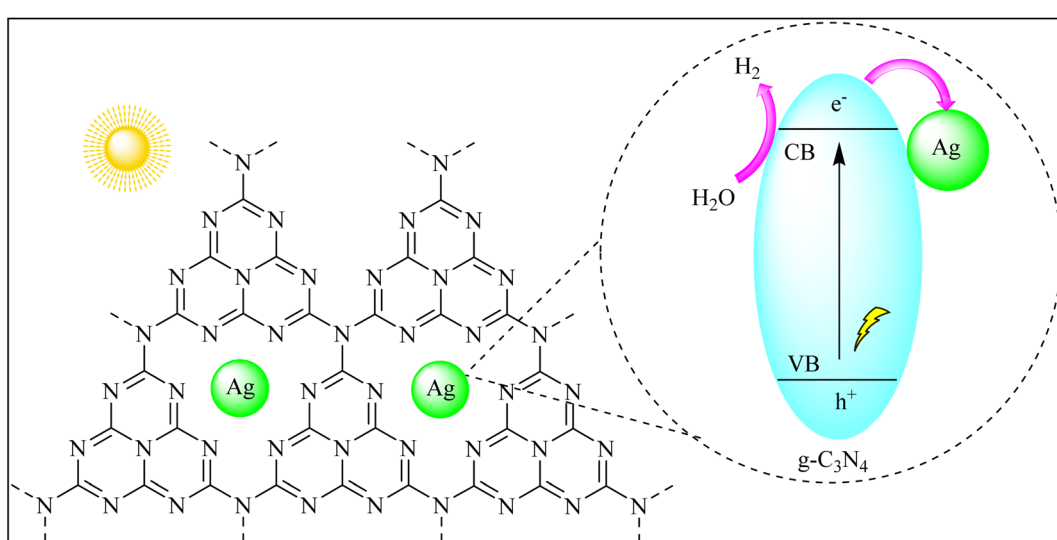
Samaniego-Benitez *et al.* created a  $\text{g-C}_3\text{N}_4/\text{NiS}$  hybrid photocatalyst through a combination of thermal decomposition and hydrothermal techniques. This hybrid material exhibited a remarkable hydrogen production yield of 1230 mmol  $\text{H}_2/\text{h}$ , which was significantly higher than that achieved by  $\text{g-C}_3\text{N}_4$  and  $\text{TiO}_2$  photocatalysts. The kinetic constant for this hybrid material was measured at  $307.1 \text{ h}^{-1}$ . This enhanced photocatalytic activity can be attributed to the reduced rate of electron–hole recombination, which results from the mixed phases found in the hybrid structure of the photocatalyst, as depicted in Fig. 9(a).<sup>90</sup>

Li *et al.* used  $\text{g-C}_3\text{N}_4$  and Ag/AgBr NPs as the carrier and co-catalyst to create  $\text{g-C}_3\text{N}_4/\text{Ag}/\text{AgBr}$  heterojunctions through solvothermal technology. They analyzed the samples'

characteristics and studied their hydrogen evolution catalytic activity through water splitting. The catalyst exhibited the best performance with low overvoltage, a shallow Tafel slope, and high catalytic activity, even without a Pt co-catalyst. This heterojunction photocatalyst demonstrated excellent photostability and recyclability. The addition of Ag/AgBr NPs to two-dimensional  $\text{g-C}_3\text{N}_4$  nanosheets enhanced their photo-response and photocatalytic activity as depicted in Fig. 9(b).<sup>91</sup>

Zhu and co-authors devised a distinctive  $\text{Mn}_3\text{O}_4/\text{g-C}_3\text{N}_4$  p–n heterojunction through an *in situ* growth method. This heterojunction notably enhances the light absorption capacity of  $\text{g-C}_3\text{N}_4$ . The resulting photocatalyst exhibits remarkable efficiency in the hydrogen evolution reaction (HER), achieving a rate of approximately  $2700 \mu\text{mol g}^{-1} \text{ h}^{-1}$  for wavelengths beyond 420 nm and maintaining stability over 15 hours of continuous  $\text{H}_2$  production. The  $\text{Mn}_3\text{O}_4/\text{g-C}_3\text{N}_4$  system also displays elevated external quantum efficiencies (EQEs) at various wavelengths. Additionally, it adeptly catalyzes both  $\text{H}_2$  and  $\text{O}_2$  evolution under simulated sunlight and accomplishes overall water splitting to generate  $\text{H}_2$  and  $\text{O}_2$  products in a stoichiometric molar ratio of 2 : 1. This research introduces a straightforward method for crafting high-performance  $\text{g-C}_3\text{N}_4$ -based heterostructure materials for efficient photocatalytic overall water splitting, as depicted in Fig. 10.<sup>92</sup>

The case study highlights diverse approaches to enhancing photocatalytic hydrogen production using  $\text{g-C}_3\text{N}_4$  composites (Table 2). While Han *et al.*'s Ag-based composites leverage

Fig. 8 Photocatalytic hydrogen production with  $\text{Ag}/\text{g-C}_3\text{N}_4$  composites under visible light.

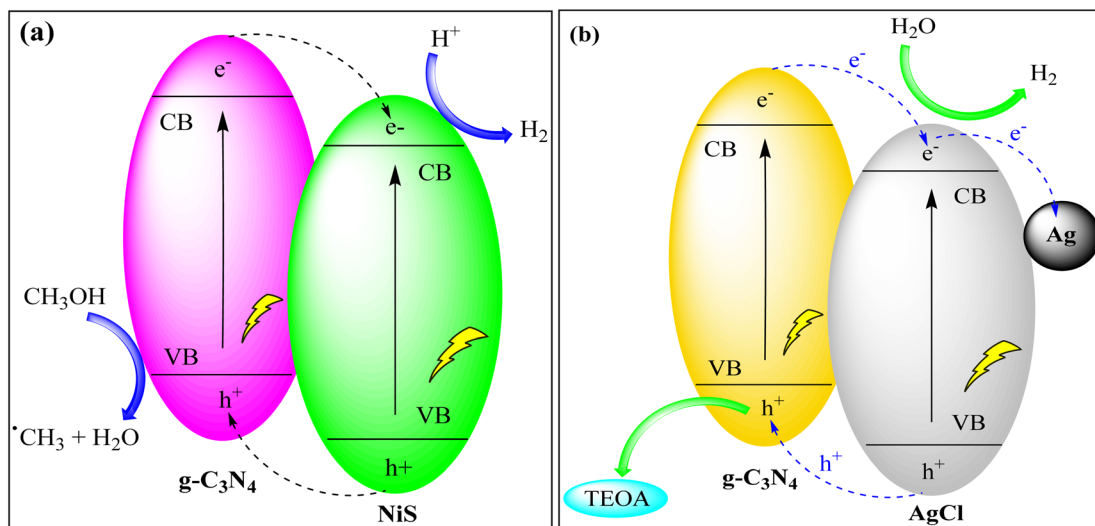


Fig. 9 (a) Hydrogen production via  $\text{g-C}_3\text{N}_4/\text{NiS}$  photocatalyst under UV light irradiation and (b) photocatalytic hydrogen production via the  $\text{Ag@g-C}_3\text{N}_4/\text{AgCl}$  heterostructure.

metallic Ag and active sites for improved charge separation, Samaniego-Benitez *et al.*'s  $\text{g-C}_3\text{N}_4/\text{NiS}$  hybrid focuses on minimizing electron-hole recombination through mixed phases. Li *et al.*'s  $\text{g-C}_3\text{N}_4/\text{Ag/AgBr}$  heterojunction demonstrates the effectiveness of incorporating co-catalysts for superior catalytic activity and stability, while Zhu *et al.*'s  $\text{Mn}_3\text{O}_4/\text{g-C}_3\text{N}_4$  p–n heterojunction introduces a unique strategy with high efficiency and overall water splitting capabilities under simulated

sunlight. These studies collectively underscore the versatility and innovation in tailoring  $\text{g-C}_3\text{N}_4$ -based photocatalysts for enhanced hydrogen evolution.

In the quest for clean and renewable energy sources,  $\text{g-C}_3\text{N}_4$  emerges as a key player in the vital endeavor of hydrogen production through water splitting. Its unique ability to harvest solar energy and catalyze the conversion of water into hydrogen represents a sustainable solution with far-reaching

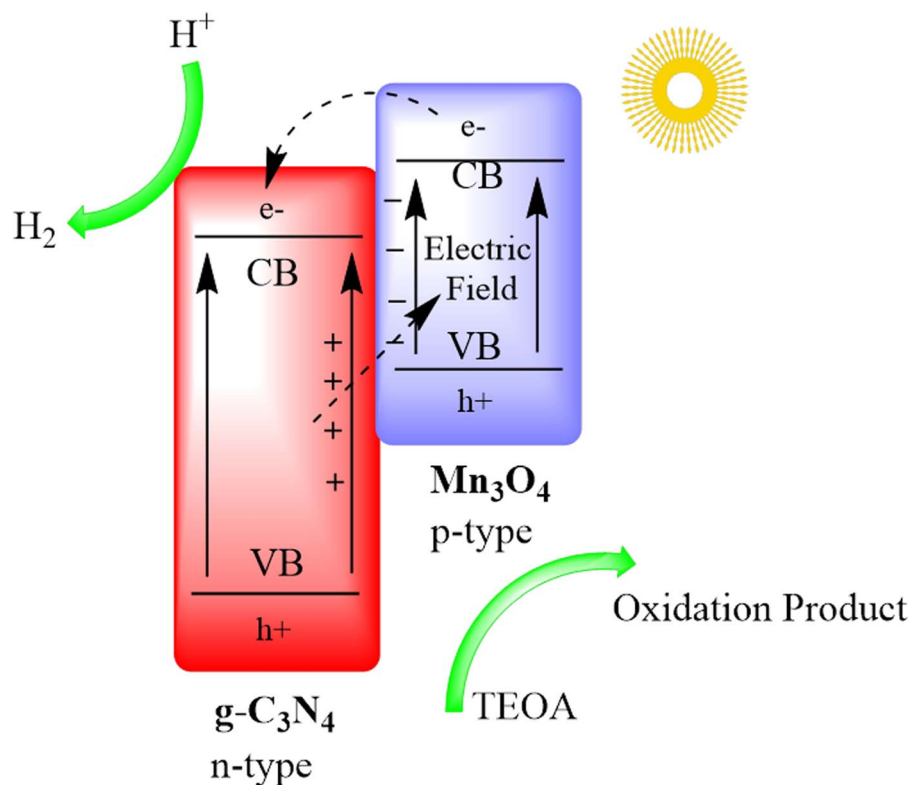


Fig. 10  $\text{Mn}_3\text{O}_4/\text{g-C}_3\text{N}_4$  based p–n heterojunction for hydrogen production.

Table 2 Photocatalytic hydrogen production via  $\text{g-C}_3\text{N}_4$  based catalysts

| Entry | Catalyst                                       | Conditions   | $\text{H}_2$ productivity/<br>$\mu\text{mol g}^{-1} \text{h}^{-1}$ | Reference material<br>$\text{H}_2$ productivity/ $\mu\text{mol g}^{-1} \text{h}^{-1}$ | Enhancement relative<br>to conventional $\text{g-C}_3\text{N}_4$ | Ref. |
|-------|--|--|--|---|--|------|
| 1     | $\text{Ag/g-C}_3\text{N}_4$                    | 300 W Xe lamp ( $\lambda > 420 \text{ nm}$ )             | 153.33   | 33.49   | 4.6  | 89   |
| 2     | $\text{NiS/g-C}_3\text{N}_4$                   | UV pen ray Hg lamp<br>(254 nm, 4.4 mW $\text{cm}^{-2}$ ) | 307.5  | 277.5   | 1.10   | 90   |
| 3     | $\text{g-C}_3\text{N}_4\text{-Ag/AgBr}$        | 300 W Xe lamp  | 47.84  | NA  | NA   | 91   |
| 4     | $\text{Mn}_3\text{O}_4/\text{g-C}_3\text{N}_4$ | 300 W Xe lamp ( $\lambda > 420 \text{ nm}$ )             | 2700   | NA  | NA   | 92   |

implications. As we look toward a future fueled by clean energy,  $\text{g-C}_3\text{N}_4$  offers a promising pathway, contributing not only to the mitigation of climate change but also to the establishment of a hydrogen-based economy. With the absorption of each photon and splitting of each water molecule,  $\text{g-C}_3\text{N}_4$  takes us one step closer to a world powered by abundant, eco-friendly hydrogen fuel, ushering in a new era of energy sustainability.

### 5.3 Water purification and treatment

One of the most critical applications of  $\text{g-C}_3\text{N}_4$  is in water purification and treatment. Its photocatalytic prowess enables the degradation of organic pollutants and the removal of toxic heavy metals from contaminated water sources. Specific examples include the degradation of dyes, pharmaceuticals, and pesticides, as well as the removal of heavy metals like chromium and lead. By providing a sustainable and efficient means of water remediation,  $\text{g-C}_3\text{N}_4$  contributes to safer and cleaner water resources.<sup>93</sup>

Ding *et al.* successfully synthesized a nanocomposite of magnetic graphene oxide (mGO) and graphitic carbon nitride ( $\text{g-C}_3\text{N}_4$ ), denoted as mGCN, for the photoreduction of U(vi) in wastewater using visible LED light irradiation. mGCN exhibited high photocatalytic activity, reusability, and selectivity for U(vi) reduction. The photoreduction process achieved a remarkable U(vi) extraction capacity of  $2880.6 \text{ mg g}^{-1}$ . Mechanistic studies revealed that U(vi) was converted to metastudtite during the photoreduction process. This research contributes to the advancement of photocatalytic methods for addressing uranium wastewater treatment, as illustrated in Fig. 11.<sup>94</sup>

Gnana Prakash *et al.* developed  $\text{g-C}_3\text{N}_4$  and  $\text{g-C}_3\text{N}_4/\text{ZnO}$  nanocomposite photocatalysts for crystal violet degradation

using melamine pyrolysis and hydrothermal methods. The nanocomposite showed superior photocatalytic efficiency (97%) compared to pristine ZnO and  $\text{g-C}_3\text{N}_4$ , with a 1.4 times higher rate constant. It exhibited excellent stability through multiple recycling tests. Hole ( $\text{h}^+$ ) species were found to be the primary drivers of crystal violet degradation. The enhanced performance of the  $\text{g-C}_3\text{N}_4/\text{ZnO}$  nanocomposite is attributed to improved visible light absorption and the formation of a heterojunction between  $\text{g-C}_3\text{N}_4$  and ZnO, promoting efficient charge carrier separation, as depicted in Fig. 12.<sup>95</sup>

Kumar and colleagues synthesized graphitic carbon nitride ( $\text{g-C}_3\text{N}_4$ ) by reducing melamine using a pyrolysis method. They then improved its characteristics to produce porous  $\text{g-C}_3\text{N}_4$  (p- $\text{g-C}_3\text{N}_4$ ) through chemical protonation. The photocatalytic performances of both materials were assessed by decomposing organic dyes under sunlight. The protonation process induced a blue-shift in the optical absorption edge of  $\text{g-C}_3\text{N}_4$ . The study demonstrated that  $\text{g-C}_3\text{N}_4$  exhibited superior photocatalytic efficiency compared to its pristine counterpart. p- $\text{g-C}_3\text{N}_4$  showed significantly enhanced degradation efficiency for various dyes under sunlight, attributed to an increased surface area that exposed more active sites for dye degradation, as depicted in Fig. 13.<sup>96</sup>

Comparing the three studies (Table 3), Ding *et al.*'s mGCN nanocomposite stands out for its effective photoreduction of U(vi) in wastewater, showcasing high activity, reusability, and selectivity with a remarkable extraction capacity. Gnana Prakash *et al.*'s  $\text{g-C}_3\text{N}_4/\text{ZnO}$  nanocomposite demonstrates superior photocatalytic efficiency in crystal violet degradation, attributed to enhanced visible light absorption and efficient charge carrier separation in the heterojunction structure. Kumar *et al.*'s work

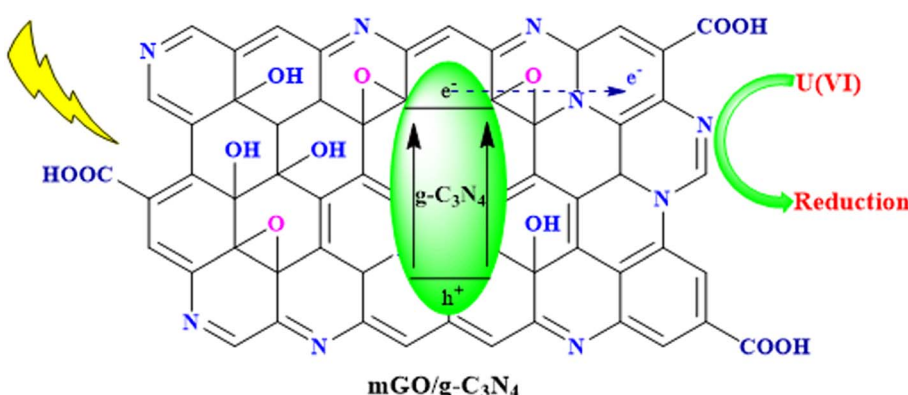


Fig. 11 Photocatalytic reduction of U(vi) in wastewater using the mGO/g-C<sub>3</sub>N<sub>4</sub> nanocomposite under visible LED light irradiation.



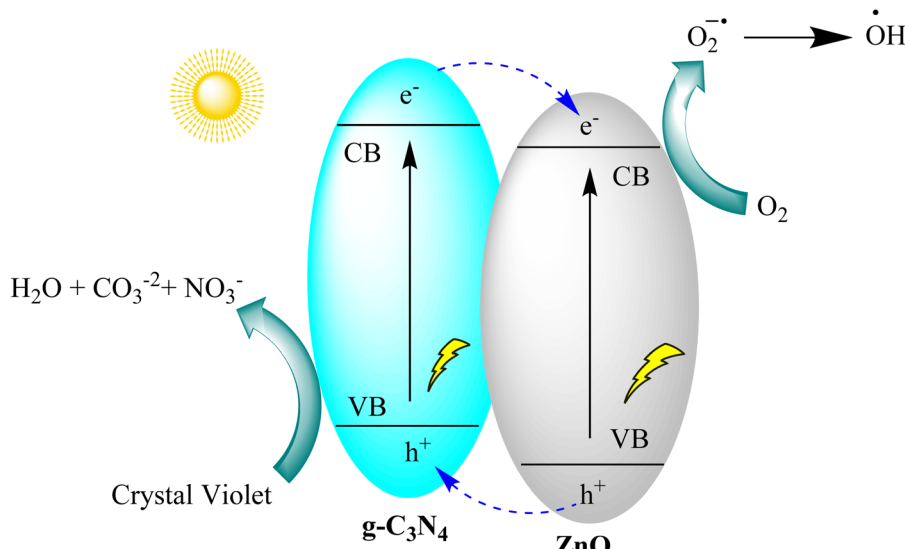


Fig. 12  $\text{g-C}_3\text{N}_4/\text{ZnO}$  heterostructure for organic dye degradation under visible light irradiation.

focuses on porous  $\text{g-C}_3\text{N}_4$ , highlighting its superior photocatalytic efficiency for dye degradation under sunlight due to increased surface area and exposure of active sites. These studies collectively underscore the versatility of  $\text{g-C}_3\text{N}_4$ -based photocatalysts for diverse applications in environmental remediation.

In the realm of water purification and treatment,  $\text{g-C}_3\text{N}_4$  stands as a beacon of hope, offering a sustainable and efficient solution to the pressing challenges of water pollution. Its ability to harness the power of sunlight to degrade organic pollutants and remove toxic heavy metals from contaminated water sources represents a transformative approach to safeguarding one of our most precious resources. As we confront the ever-growing concerns of water quality and scarcity,  $\text{g-C}_3\text{N}_4$  paves the way

for cleaner and safer water supplies. With each photocatalytic reaction, it exemplifies the potential for science and innovation to address the critical issue of water pollution, ensuring that future generations will inherit a world with access to clean and potable water. In the intersection of environmental stewardship and technological advancement,  $\text{g-C}_3\text{N}_4$ 's role in water purification and treatment is not merely a solution; it is a promise of a more sustainable and water-secure future.

#### 5.4 Air purification and pollutant removal

The degradation of volatile organic compounds (VOCs) and the removal of noxious gases from the atmosphere are essential for improving air quality.  $\text{g-C}_3\text{N}_4$ 's photocatalytic activity extends to air purification applications, where it effectively degrades VOCs

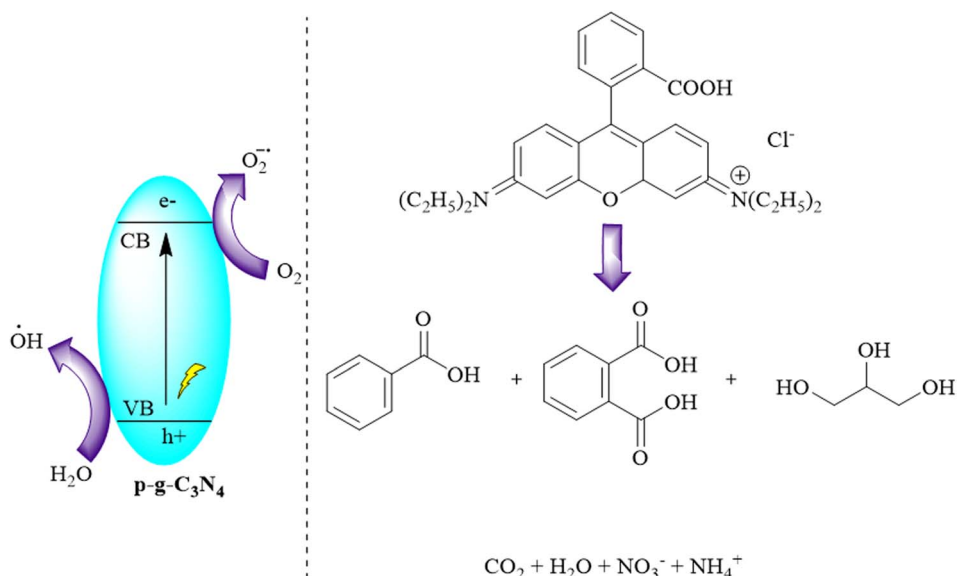


Fig. 13 Porous  $\text{g-C}_3\text{N}_4$  for photocatalytic dye degradation.

Table 3 Pollutant degradation via  $\text{g-C}_3\text{N}_4$  based catalysts

| Entry | Catalyst                            | Organic dye                                     | Conditions   | Removal efficiency (%) | Reference material efficiency (%) | Ref. |
|-------|-------------------------------------|---|--|------------------------|-----------------------------------|------|
| 1     | $\text{mGO/g-C}_3\text{N}_4$        | NA  | 5 mg catalyst, methanol, 30 mL<br>20 mg $\text{L}^{-1}$ $\text{U}(\text{vi})$ solution, 8 W LED lamp | 96                     | NA                                | 94   |
| 2     | $\text{g-C}_3\text{N}_4/\text{ZnO}$ | Crystal violet                                  | 25 mg of catalyst and 25 mL of 20 ppm<br>crystal violet solution, solar irradiation                  | 97                     | 88                                | 95   |
| 3     | $\text{p-g-C}_3\text{N}_4$          | Crystal violet<br>Methylene blue<br>Rhodamine-B | 25 mg catalyst, 25 mL (20 mg $\text{L}^{-1}$ ) of an<br>aqueous solution, sunlight irradiation       | 98<br>99<br>93         | 92<br>83<br>32                    | 96   |

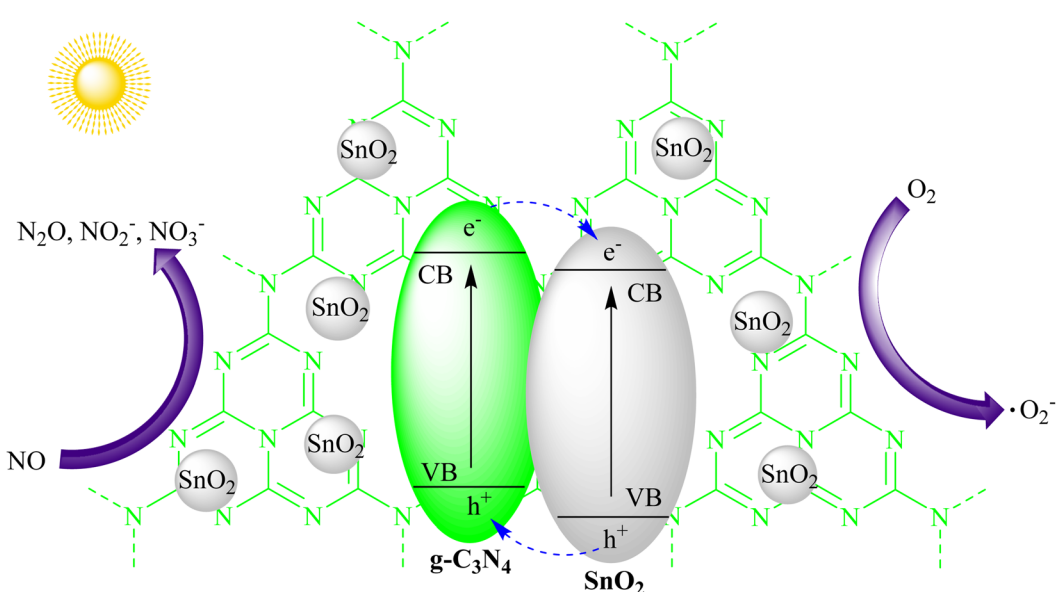
like formaldehyde, toluene, and xylene. Additionally, it can facilitate the conversion of harmful gases like nitrogen oxides ( $\text{NO}_x$ ) into less harmful compounds. The utilization of  $\text{g-C}_3\text{N}_4$  in air purification technologies helps combat air pollution and promote healthier living environments.

Zhou and their team successfully incorporated  $\text{SnO}_2$  quantum dots into graphitic carbon nitride ( $\text{g-C}_3\text{N}_4$ ) via a simple synthesis method. This led to the development of photocatalysts that generated minimal  $\text{NO}_2$  and achieved a 32% NO removal rate when exposed to visible light for 30 minutes. The attachment of  $\text{SnO}_2$  quantum dots not only improved the photocatalysts' ability to reduce  $\text{NO}_2$  but also enhanced the transfer of photogenerated carriers, improving NO removal. This study provided an accessible way to combine a wide bandgap semiconductor ( $\text{SnO}_2$ ) with strong photo-oxidation capabilities and layered  $\text{g-C}_3\text{N}_4$ , which responds well to visible light for NO removal. Future research is needed to eliminate  $\text{NO}_2$  byproducts in the photocatalytic NO removal process, as shown in Fig. 14.<sup>97</sup>

Huang *et al.* created a  $\text{g-C}_3\text{N}_4/\text{TiO}_2$  composite coating for removing  $\text{NO}_x$  in ambient air. They applied it directly to roads using  $\text{TiO}_2$  hydrosol, eliminating the need for dispersants or binders. The coating had strong adhesion, easy regeneration,

and light-induced superhydrophilicity, making it suitable for long-term use. It achieved daily NO and  $\text{NO}_x$  reductions of 59.0% and 27.8%, respectively, and higher rates during morning and afternoon hours with weak sunlight. This was due to the coating's broad visible light absorption, critical for pollution reduction. Outdoor results showed that  $\text{NO}_x$  removal depended on solar irradiation and pollutant concentration, with the latter being more important due to reaction kinetics. In conclusion, the  $\text{g-C}_3\text{N}_4/\text{TiO}_2$  composite and spraying method offer a simple and effective way to create photocatalytic pavement for air purification as shown in Fig. 15.<sup>98,99</sup>

You and collaborators synthesized  $\text{MgO}@\text{g-C}_3\text{N}_4$  heterojunctions through a one-step pyrolysis process involving commercial  $\text{MgO}$  and urea, leading to a significant enhancement in photocatalytic efficiency. The 3%  $\text{MgO}@\text{g-C}_3\text{N}_4$  sample exhibited the highest efficiency in NO photodegradation at 75.4%. However, beyond 3%  $\text{MgO}$ , the efficiency experienced a decline. The heterojunction structure, resulting from the combination of  $\text{MgO}$  and  $\text{g-C}_3\text{N}_4$ , played a crucial role in improving appearance quantum efficiency and prolonging electron recombination, ultimately contributing to superior NO photodegradation. The composite also demonstrated favorable conversion of NO to  $\text{NO}_2$  and other by-products. Notably, the 3%

Fig. 14  $\text{g-C}_3\text{N}_4/\text{SnO}_2$  heterostructure for removal of NO under visible light irradiation.

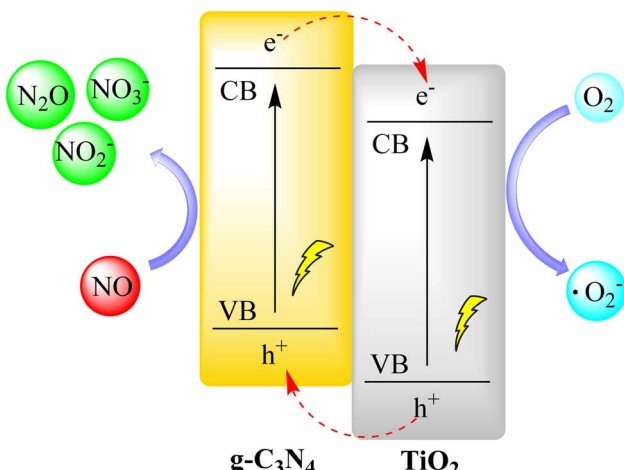


Fig. 15 g-C<sub>3</sub>N<sub>4</sub>/TiO<sub>2</sub> heterostructure for removal of NO under visible light irradiation

$\text{MgO}@\text{g-C}_3\text{N}_4$  maintained high reusability after five cycles, with only a modest 7.1% decrease in efficiency. Characterization techniques confirmed the presence of  $\text{MgO}$  and its impact on optical properties, suggesting scalability for future applications. Overall, the study provides valuable insights into optimizing  $\text{MgO}@\text{g-C}_3\text{N}_4$  photocatalysis, as illustrated in Fig. 16.<sup>100</sup>

Comparing the three studies (Table 4), Zhou *et al.*'s incorporation of  $\text{SnO}_2$  quantum dots into  $\text{g-C}_3\text{N}_4$  showcases a simple method for developing photocatalysts with a 32% NO removal rate under visible light. This approach effectively combines the strong photo-oxidation capabilities of  $\text{SnO}_2$  with the layered structure of  $\text{g-C}_3\text{N}_4$ , demonstrating potential for NO reduction. Huang *et al.*'s  $\text{g-C}_3\text{N}_4/\text{TiO}_2$  composite coating directly applied to roads offers a practical and efficient solution for  $\text{NO}_x$  removal from ambient air, achieving daily reductions and demonstrating adaptability to varying sunlight conditions. You and collaborators' synthesis of  $\text{MgO}@g\text{-C}_3\text{N}_4$  heterojunctions provides valuable insights into optimizing photocatalysis for

NO degradation, emphasizing the importance of the composite structure for enhanced efficiency and reusability. These studies collectively contribute to the development of effective and accessible photocatalytic methods for NO and  $\text{NO}_x$  removal in different environmental contexts.

In the realm of air purification and the removal of noxious pollutants,  $g\text{-C}_3\text{N}_4$  emerges as a powerful agent of change, working tirelessly to enhance the quality of the air we breathe. Its remarkable photocatalytic abilities, adept at degrading volatile organic compounds (VOCs) and transforming harmful gases, have the potential to combat air pollution and improve the health of our environments. As the world grapples with the consequences of urbanization and industrialization,  $g\text{-C}_3\text{N}_4$  offers a glimmer of hope for cleaner and healthier air. With each chemical bond broken and each pollutant neutralized, it embodies the promise of harnessing sustainable technologies to restore the purity of our atmosphere. In the ongoing battle against air pollution,  $g\text{-C}_3\text{N}_4$ 's role is not merely that of a catalyst; it is a symbol of our collective commitment to cleaner, more breathable air, ensuring a future where all can thrive in an environment free from harmful pollutants.

## 5.5 Solar-driven carbon dioxide reduction

Addressing the challenge of increasing carbon dioxide (CO<sub>2</sub>) levels in the atmosphere necessitates innovative approaches for its conversion into valuable products. g-C<sub>3</sub>N<sub>4</sub> has demonstrated promise in the solar-driven reduction of CO<sub>2</sub> into hydrocarbons and other valuable chemicals. This application holds immense potential for both mitigating climate change and producing sustainable feedstocks for various industries.

Li *et al.* created a versatile Pt/In<sub>2</sub>O<sub>3</sub>/g-C<sub>3</sub>N<sub>4</sub> catalyst using precise assembly techniques. This catalyst efficiently produced formic acid (HCOOH) during visible-light-driven CO<sub>2</sub> reduction by synergistically promoting hydrogen generation, CO<sub>2</sub> activation, and minimizing electron-hole recombination. It also had a long operational life due to stability and prevented Pt leaching. This work offers a promising method to design multi-functional catalysts for high-yield, room-temperature, and normal-pressure photocatalytic CO<sub>2</sub> reduction as depicted in Fig. 17.<sup>101</sup>

Khan *et al.* used a CuO/g-C<sub>3</sub>N<sub>4</sub> photocatalyst to produce methanol *via* photoelectrochemical reduction of CO<sub>2</sub>. The CuO/g-C<sub>3</sub>N<sub>4</sub> photocathode outperformed others, showing a tenfold increase in the photocurrent response. It had high incident photon-to-current efficiency and significantly increased methanol production. The photocathode also had improved faradaic and quantum efficiency compared to other configurations. The study discussed the CO<sub>2</sub>-to-methanol conversion mechanism in detail, as shown in Fig. 18.<sup>102</sup>

Yu *et al.* successfully created a Z-scheme binary composite photocatalytic system by combining g-C<sub>3</sub>N<sub>4</sub> and ZnO through a simple calcination process, using affordable precursors, urea, and zinc nitrate hexahydrate. This composite exhibited improved light absorption in the visible spectrum compared to pure g-C<sub>3</sub>N<sub>4</sub>, thanks to the introduction of defect states within the g-C<sub>3</sub>N<sub>4</sub> due to the interference of ZnO crystallization.

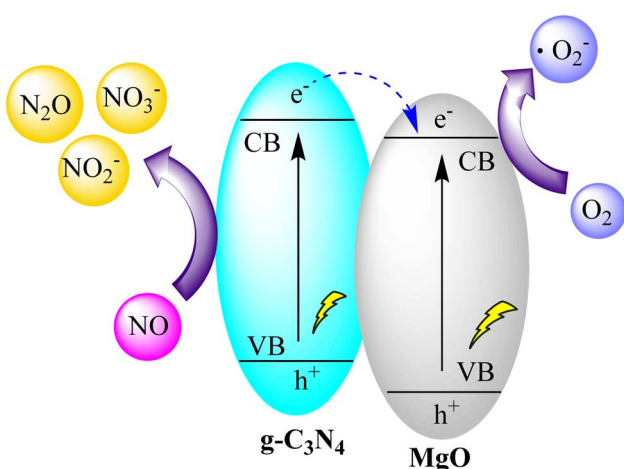
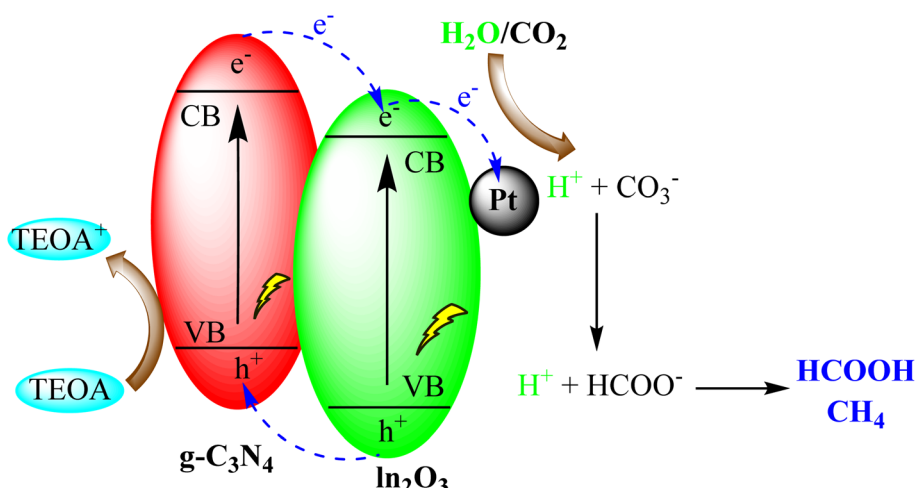


Fig. 16 MgO@g-C<sub>3</sub>N<sub>4</sub> for degradation of NO under visible light irradiation.

Table 4 Air pollutant degradation via  $\text{g-C}_3\text{N}_4$ -based catalytic systems

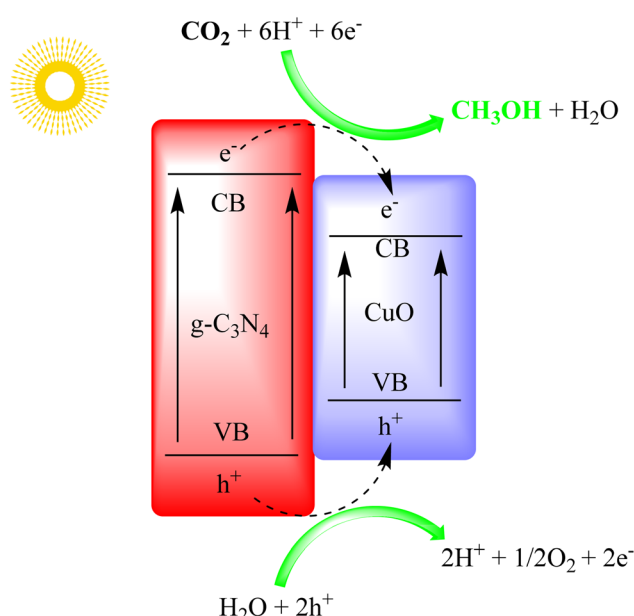
| Entry | Catalyst  | Conditions   | NO removal efficiency (%) | Reference material efficiency (%) | Ref. |
|-------|---|--|---------------------------|-----------------------------------|------|
| 1     | $\text{SnO}_2$ quantum dots on $\text{g-C}_3\text{N}_4$ | 0.4 g catalyst, NO concentration 600 ppb, 150 W tungsten halogen lamp ( $\lambda > 420$ nm)  | 32                        | 19                                | 97   |
| 2     | $\text{g-C}_3\text{N}_4/\text{TiO}_2$                   | 5 L Teflon air bag (232-05, Tedlar®) for 45 min with a height of 1.0–1.5 m from the ground by using a sampling pump with a flow rate of $0.1 \text{ L min}^{-1}$ | 38.9                      | 23.5 ( $\text{TiO}_2$ )           | 98   |
| 3     | $\text{MgO}@\text{g-C}_3\text{N}_4$                     | 0.2 g catalyst, NO concentration 500 ppb, 10 mL water, $80^\circ\text{C}$ , 300 W xenon lamp   | 75.4                      | 62.8                              | 100  |

Fig. 17 Pt/In<sub>2</sub>O<sub>3</sub>/g-C<sub>3</sub>N<sub>4</sub> heterostructure for CO<sub>2</sub> reduction under visible light irradiation.

Notably, the  $\text{g-C}_3\text{N}_4/\text{ZnO}$  photocatalyst displayed a 2.3-fold increase in its ability to catalyze the conversion of CO<sub>2</sub> into CH<sub>3</sub>OH while maintaining selectivity, as shown in Fig. 19. This indicates the promising potential of this composite for efficient CO<sub>2</sub> reduction applications.<sup>103</sup>

Pant and co-authors presented a straightforward approach for crafting a conjugated organic-inorganic hybrid photocatalyst ( $\text{TiO}_2/\text{g-C}_3\text{N}_4$ ) through sol-gel synthesis followed by conventional pyrolysis. The heterostructure formed by TiO<sub>2</sub> and g-C<sub>3</sub>N<sub>4</sub> efficiently facilitated the separation of electrons and holes, as evidenced by their respective band edge positions. This TiO<sub>2</sub> and g-C<sub>3</sub>N<sub>4</sub> heterostructure exhibited a type II heterojunction, renowned for promoting enhanced charge separation and mitigating charge recombination. The augmented charge separation contributed to an increased photoreduction of CO<sub>2</sub>, yielding valuable methanol as the photo-reduced product. The composite catalysts demonstrated a higher methanol yield ( $31.7 \mu\text{mol g}^{-1}$ ) compared to the individual components. The study underscores the crucial role of charge separation in a straightforward heterostructure catalyst, leading to heightened product formation through CO<sub>2</sub> reduction under a visible light source, as depicted in Fig. 20.<sup>104</sup>

Li *et al.*'s versatile Pt/In<sub>2</sub>O<sub>3</sub>/g-C<sub>3</sub>N<sub>4</sub> catalyst stands out for its ability to efficiently produce formic acid during visible-light

Fig. 18 g-C<sub>3</sub>N<sub>4</sub>/CuO heterostructure for photo electrocatalytic CO<sub>2</sub> reduction under visible light irradiation.

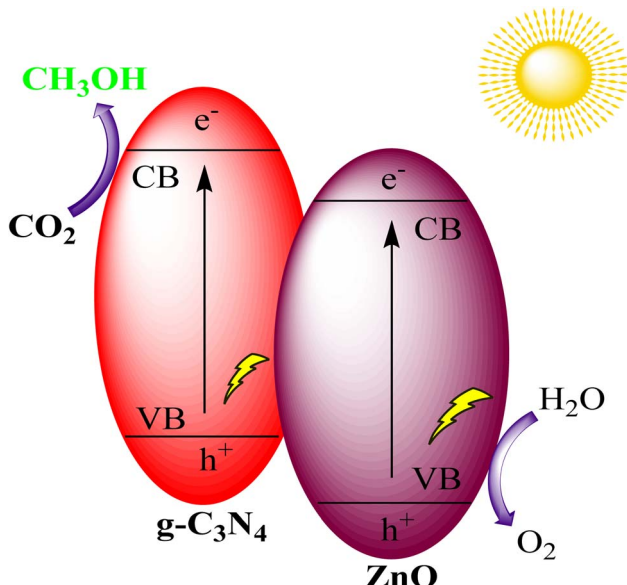


Fig. 19  $\text{g-C}_3\text{N}_4/\text{ZnO}$  heterostructure for photocatalytic  $\text{CO}_2$  reduction under visible light irradiation.

driven  $\text{CO}_2$  reduction. The catalyst's multifunctionality, promoting hydrogen generation,  $\text{CO}_2$  activation, and minimizing electron–hole recombination, demonstrates promise for high-yield, room-temperature, and normal-pressure photocatalytic  $\text{CO}_2$  reduction. Khan *et al.*'s  $\text{CuO}/\text{g-C}_3\text{N}_4$  photocathode excels in producing methanol *via* photoelectrochemical reduction of  $\text{CO}_2$ , showcasing a tenfold increase in the photocurrent response and improved faradaic and quantum efficiency. Yu *et al.*'s Z-scheme  $\text{g-C}_3\text{N}_4/\text{ZnO}$  composite offers enhanced light absorption and a 2.3-fold increase in catalyzing  $\text{CO}_2$  conversion to  $\text{CH}_3\text{OH}$ , highlighting its potential for efficient  $\text{CO}_2$  reduction. Pant and co-authors'  $\text{TiO}_2/\text{g-C}_3\text{N}_4$  heterostructure demonstrates the importance of charge separation, yielding higher methanol production compared to individual components. These studies collectively contribute valuable insights into designing

efficient photocatalysts for diverse applications in  $\text{CO}_2$  reduction (Table 5).

In the ambitious endeavor to combat climate change and harness solar energy,  $\text{g-C}_3\text{N}_4$  emerges as a beacon of innovation and sustainability in the realm of solar-driven carbon dioxide reduction. Its capacity to convert the ubiquitous greenhouse gas, carbon dioxide, into valuable hydrocarbons and chemicals represents a profound stride towards a carbon-neutral future. As we confront the urgent need to reduce carbon emissions and transition to renewable energy sources,  $\text{g-C}_3\text{N}_4$  embodies the promise of a cleaner, more sustainable world. With the absorption of each photon and transformation of each carbon dioxide molecule, it not only mitigates climate change but also offers a glimpse into the boundless possibilities of harnessing solar energy for a greener tomorrow. In the intersection of environmental preservation and renewable energy,  $\text{g-C}_3\text{N}_4$ 's role in solar-driven carbon dioxide reduction is a testament to our commitment to a more sustainable, carbon-conscious, and brighter future.

## 5.6 Solar fuel cells

Solar fuel cells represent a vital component of the renewable energy landscape.  $\text{g-C}_3\text{N}_4$ 's ability to generate hydrogen and other energy carriers through photocatalysis aligns with the development of solar fuel cells. These cells can store and utilize solar energy for power generation and transportation, reducing reliance on fossil fuels and minimizing greenhouse gas emissions.

Liu *et al.* developed a visible-light-driven photocatalytic fuel cell (PFC) that efficiently degrades tetracycline hydrochloride (TC) and generates electricity in a single reactor. The PFC used paired stainless-steel mesh electrodes loaded with specific catalysts under different conditions, with and without visible light. With visible light, TC removal was highly effective (97.3% in 90 minutes), with a cell voltage of 0.98 V and  $24 \text{ W m}^{-2}$  power density. Simultaneous removal of chemical oxygen demand (COD) and total organic carbon (TOC) was notable, driven by the anodic  $\text{g-C}_3\text{N}_4/\text{Fe}^0$  (1%)/ $\text{TiO}_2$  component. Without light, performance dropped significantly, but the PFC continued to operate as a self-driven system, degrading pollutants. The PFC maintained its performance over multiple cycles with light, offering potential for wastewater treatment. In the dark, it still generated electricity but at reduced capacity. This research shows promise for efficient pollutant removal and energy recovery in wastewater treatment, as shown in Fig. 21.<sup>105,106</sup>

Zhang *et al.* significantly enhanced the performance of carbon-based perovskite solar cells without a hole-transporting material (HTM). They achieved a power conversion efficiency (PCE) above 14% by introducing  $\text{g-C}_3\text{N}_4$  doping and an  $\text{Al}_2\text{O}_3$  insulating layer, as depicted in Fig. 22.  $\text{g-C}_3\text{N}_4$  improved the perovskite film quality, and with just 0.5 wt%  $\text{g-C}_3\text{N}_4$  doping, the PCE increased to 12.85%. The  $\text{Al}_2\text{O}_3$  insulating layer enhanced open-circuit voltage ( $V_{oc}$ ) and further increased PCE to 14.34% by reducing recombination at the ETM/perovskite interface. The resulting device demonstrated good stability, offering potential for cost-effective, high-performance

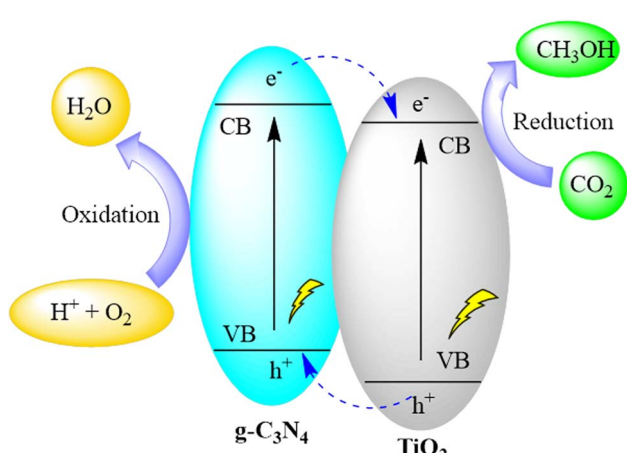


Fig. 20  $\text{g-C}_3\text{N}_4/\text{TiO}_2$  heterostructure for photocatalytic  $\text{CO}_2$  reduction under visible light irradiation.



Table 5 Solar-driven carbon dioxide reduction via  $g\text{-C}_3\text{N}_4$ -based catalytic systems

| Entry | Catalyst   | Conditions  | Productivity   | Reference material                             | Ref. |
|-------|--|---|--|--|------|
| 1     | Pt/In <sub>2</sub> O <sub>3</sub> / $g\text{-C}_3\text{N}_4$ | 20 mg catalyst, 1 atm CO <sub>2</sub> , 10 mL H <sub>2</sub> O, 1 mL TEOA, 35 °C, 4 h, 3 W LED (420 nm)       | HCOOH – 63.1, CH <sub>4</sub> – 7.907 ( $\mu\text{mol g}^{-1} \text{h}^{-1}$ ) | NA   | 101  |
| 2     | CuO/ $g\text{-C}_3\text{N}_4$                                | (Nafion/CuO/ $g\text{-C}_3\text{N}_4$ ), NaHCO <sub>3</sub> (0.1 M), bias potential illumination              | 25.1 ( $\mu\text{mol L}^{-1} \text{cm}^{-2}$ )                                 | 5.92 ( $\mu\text{mol L}^{-1} \text{cm}^{-2}$ ) | 102  |
| 3     | ZnO/ $g\text{-C}_3\text{N}_4$                                | 100 mg sample in 10 mL deionized water, 80 °C, 0.12 g NaHCO <sub>3</sub> , 0.25 mL 4 M HCl, 300 W Xe arc lamp | 0.60 ( $\mu\text{mol g}^{-1} \text{h}^{-1}$ )                                  | 0.26 ( $\mu\text{mol g}^{-1} \text{h}^{-1}$ )  | 103  |
| 4     | TiO <sub>2</sub> / $g\text{-C}_3\text{N}_4$                  | 0.2 g of catalyst, high purity CO <sub>2</sub> , 0.2 g of catalyst, 200 mL of 0.1 M NaOH, 250 W halogen lamp  | 31.7 ( $\mu\text{mol g}^{-1}$ )  | 14.1 ( $\mu\text{mol g}^{-1}$ )                | 104  |

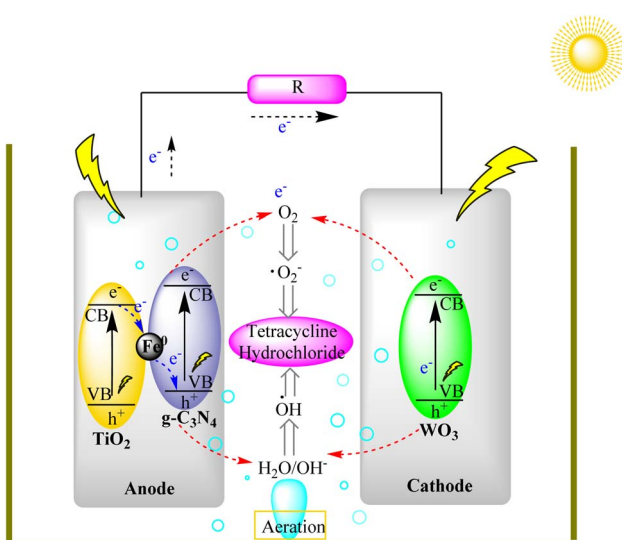


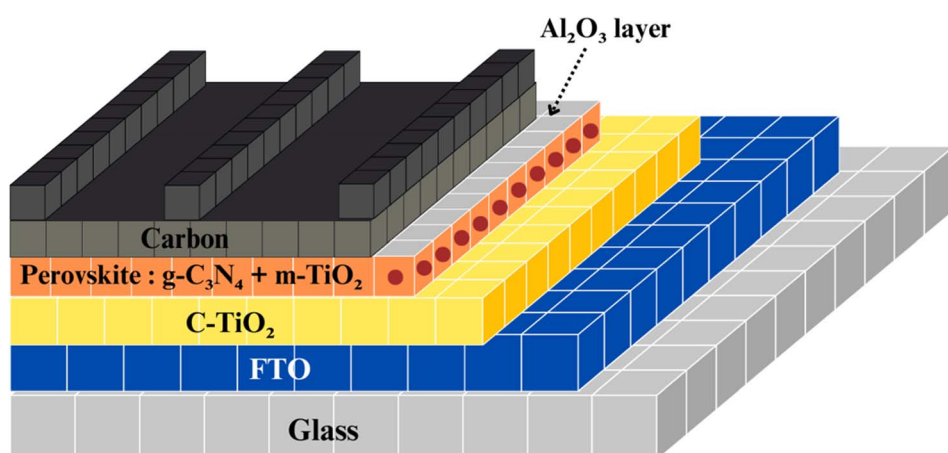
Fig. 21 Visible-light-driven photocatalytic fuel cell (PFC).

perovskite solar cells without a HTM, which could have a significant impact on the market.<sup>107,108</sup>

Wang and collaborators synthesized a Z-scheme photocatalyst, Ag<sub>3</sub>PO<sub>4</sub>@ $g\text{-C}_3\text{N}_4$ , which served as the photoanode in

a photoelectro-Fenton (PFC) system alongside Cu<sub>2</sub>O as the photocathode, as illustrated in Fig. 23. The Z-scheme structure was deliberately designed to ensure effective separation of charge carriers, thereby enhancing the overall PFC performance. Furthermore, the catalyst exhibited a high redox ability, actively participating in the degradation of organic pollutants. The electricity production of the PFC system was observed to increase with N<sub>2</sub> aeration, while O<sub>2</sub> purging proved beneficial for the photocatalytic degradation of organic pollutants. The study highlights the efficacy of the Z-scheme photocatalyst in achieving efficient charge separation and contributing to the effective degradation of organic pollutants in a PFC system.<sup>109</sup>

Liu *et al.*'s visible-light-driven photocatalytic fuel cell (PFC) efficiently degrades tetracycline hydrochloride (TC) and generates electricity, demonstrating a promising approach for simultaneous wastewater treatment and energy recovery. The PFC, operating under visible light, achieves high TC removal, and COD, and TOC reduction, showcasing its potential for sustainable wastewater treatment with electricity generation. Zhang *et al.*'s work on carbon-based perovskite solar cells with  $g\text{-C}_3\text{N}_4$  doping and an Al<sub>2</sub>O<sub>3</sub> insulating layer enhances power conversion efficiency (PCE) to over 14%, offering a cost-effective and stable solution for high-performance solar cells without a hole-transporting material (HTM). Finally, Wang *et al.*'s Z-scheme Ag<sub>3</sub>PO<sub>4</sub>@ $g\text{-C}_3\text{N}_4$  photocatalyst in a photoelectro-

Fig. 22 Al<sub>2</sub>O<sub>3</sub> layer insulated  $g\text{-C}_3\text{N}_4$  added carbon-based perovskite solar cells.

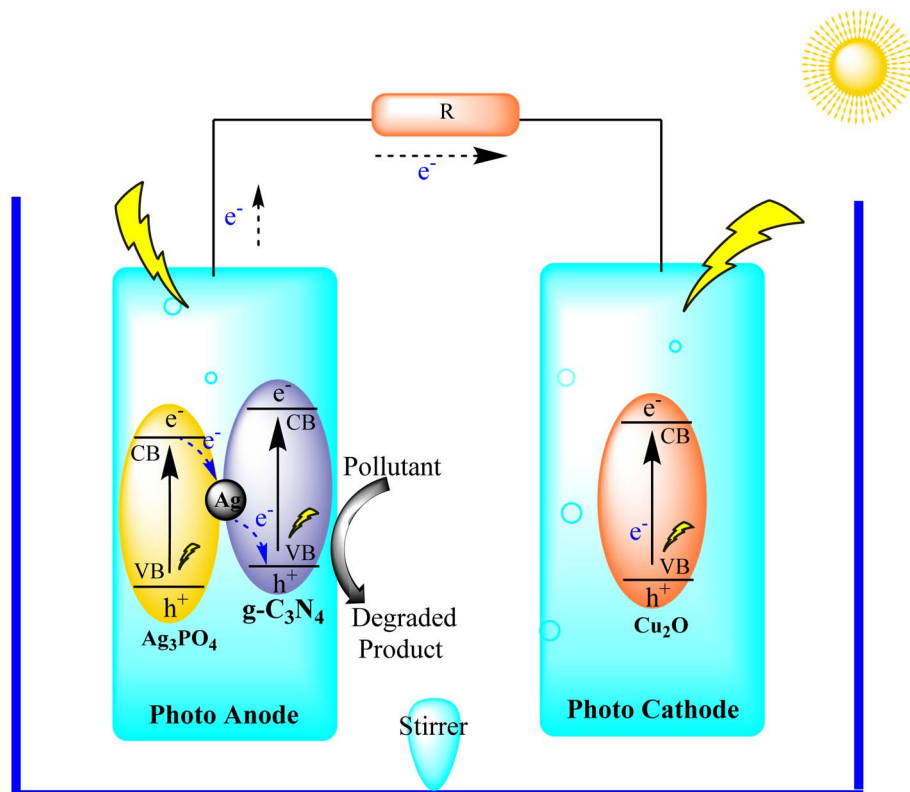


Fig. 23 Z-scheme  $\text{Ag}_3\text{PO}_4@\text{g-C}_3\text{N}_4$  photocatalyst for fuel cell synthesis.

Fenton (PFC) system demonstrates efficient charge separation and active participation in organic pollutant degradation, emphasizing its potential for environmentally friendly energy production and wastewater treatment. These studies collectively showcase the versatile applications of  $\text{g-C}_3\text{N}_4$  in advancing sustainable technologies (Table 6).

As we strive for a future powered by clean and renewable energy,  $\text{g-C}_3\text{N}_4$  emerges as a pivotal player in the realm of solar fuel cells. Its remarkable ability to harness sunlight and catalyze the conversion of solar energy into clean fuels holds the key to reducing our reliance on fossil fuels and mitigating climate change. With each electron it liberates and each hydrogen molecule it generates,  $\text{g-C}_3\text{N}_4$  not only powers our aspirations for a sustainable energy landscape but also illuminates the path

toward a greener, more promising future. In the synergy of advanced technology and environmental responsibility,  $\text{g-C}_3\text{N}_4$ 's role in solar fuel cells is a testament to our commitment to a world where clean energy sources drive our progress, ushering in an era of energy sustainability and environmental preservation.

Each of these applications of  $\text{g-C}_3\text{N}_4$  as a photocatalyst embodies a sustainable approach to addressing environmental and energy challenges. Specific case studies and examples underscore the material's effectiveness in various contexts. Furthermore, the environmental benefits, such as reduced energy consumption and lower pollutant emissions, coupled with potential economic advantages, position  $\text{g-C}_3\text{N}_4$  as a pivotal catalyst for a cleaner, more sustainable future.

Table 6  $\text{g-C}_3\text{N}_4$ -based perovskite fuel cells for photovoltaic performance

| Entry | System   | Conditions   | Current density  | Fuels   | Ref. |
|-------|--|--|--|---|------|
| 1     | $\text{Ag}_3\text{PO}_4@\text{g-C}_3\text{N}_4$  | Photocatalytic fuel cell (50 mg of photocatalyst, 10 mg $\text{L}^{-1}$ berberine chloride, 50 W Xe lamp)                          | 2.02 $\text{mA cm}^{-2}$   | Berberine chloride                            | 109  |
| 2     | FTO/c-TiO <sub>2</sub> /m-TiO <sub>2</sub> /perovskite: $\text{g-C}_3\text{N}_4$ /carbon | FTO/c-TiO <sub>2</sub> /m-TiO <sub>2</sub> /perovskite: $\text{g-C}_3\text{N}_4$ /carbon device                                    | (Perovskite) 21.5 $\text{mA cm}^{-2}$<br>(0.5 wt% $\text{g-C}_3\text{N}_4$ /perovskite) 24.0 $\text{mA cm}^{-2}$ | NA  | 107  |
| 3     | $\text{g-C}_3\text{N}_4/\text{FeO/TiO}_2$  | 0.05 g of photocatalyst, 100 mL of TC (10 mg $\text{L}^{-1}$ ), $\text{Na}_2\text{SO}_4$ (0.1 mol $\text{L}^{-1}$ ), 300 W Xe lamp | 6.06 $\mu\text{W cm}^{-2}$<br>0.067 $\mu\text{W cm}^{-2}$  | Rhodamine-B<br>Methylene blue<br>Tetracycline | 105  |



## 6. Challenges and future prospects

Graphitic carbon nitride ( $\text{g-C}_3\text{N}_4$ ) undoubtedly exhibits exceptional photocatalytic capabilities, yet several challenges warrant attention as we aim to harness its full potential. Foremost among these challenges is the need to enhance its quantum efficiency—the efficiency with which it utilizes incoming photons. Researchers are actively working to minimize electron-hole pair recombination rates and boost the overall photocatalytic conversion efficiency. Additionally, ensuring photostability over extended usage periods is critical. Factors such as photo-corrosion and aggregation can impact  $\text{g-C}_3\text{N}_4$ 's performance, necessitating the development of stable  $\text{g-C}_3\text{N}_4$  materials and protective coatings. Achieving high selectivity in complex reaction mixtures remains a formidable challenge, even though  $\text{g-C}_3\text{N}_4$  exhibits remarkable selectivity in many reactions. Fine-tuning the material's surface properties and optimizing reaction conditions continue to be areas of investigation. Finally, scaling up  $\text{g-C}_3\text{N}_4$  production from laboratory-scale to practical, large-scale applications presents logistical challenges, requiring cost-effective manufacturing methods and seamless integration into the existing infrastructure.

The future prospects for  $\text{g-C}_3\text{N}_4$  photocatalysis are exceptionally promising, driven by ongoing research and innovative strategies. The integration of advanced co-catalysts, such as metal nanoparticles or semiconductor materials, holds the potential to significantly enhance charge separation and overall photocatalytic performance. The tailoring of  $\text{g-C}_3\text{N}_4$  materials with specific structural and electronic properties optimized for various applications is another exciting avenue of exploration, allowing for custom-designed photocatalysts. These developments pave the way for tailored solutions to environmental and energy challenges. Moreover, the integration of  $\text{g-C}_3\text{N}_4$  photocatalysis with solar cell technologies in tandem or integrated systems offers the possibility of continuous and efficient energy conversion. The exploration of  $\text{g-C}_3\text{N}_4$ 's application in environmental remediation, such as addressing emerging pollutants like pharmaceuticals and microplastics in water and air, remains an area of interest. Additionally, the concept of artificial photosynthesis systems, where  $\text{g-C}_3\text{N}_4$  plays a pivotal role in replicating natural photosynthesis for sustainable fuel production and carbon capture, holds immense promise. As the world continues to prioritize environmental sustainability and clean energy,  $\text{g-C}_3\text{N}_4$  remains poised at the forefront of these advancements, representing a cornerstone in the journey toward a greener and more sustainable future.

## 7. Conclusion

In this comprehensive review, we have delved into the multi-faceted world of graphitic carbon nitride ( $\text{g-C}_3\text{N}_4$ ) as a promising photocatalyst, exploring its diverse synthesis methods, unique structural properties, intricate photocatalytic mechanisms, and transformative applications in sustainability. We've navigated through its pivotal role in various domains, from organic transformations and hydrogen production through water splitting to water purification, air purification, solar-

driven carbon dioxide reduction, and solar fuel cells. Throughout our journey, we've highlighted the environmental and economic benefits of  $\text{g-C}_3\text{N}_4$  in these applications. As we conclude, it's evident that  $\text{g-C}_3\text{N}_4$ 's innovative potential holds the promise of a cleaner, more sustainable future, making it a beacon of hope in the intersection of science and environmental stewardship.

## Conflicts of interest

The authors declare that they have no conflict of interest.

## Acknowledgements

One of the contributing authors (CKM) wishes to extend heartfelt gratitude to the fellow authors of this review article. Their unwavering enthusiasm, dedication, and relentless efforts were instrumental in turning this comprehensive review article into the final shape.

## References

- 1 P. Li, J. A. Terrett and J. R. Zbieg, Visible-Light Photocatalysis as an Enabling Technology for Drug Discovery: A Paradigm Shift for Chemical Reactivity, *ACS Med. Chem. Lett.*, 2020, **11**, 2120–2130.
- 2 A. Xie, *et al.*, Photocatalytic Technologies for Transformation and Degradation of Microplastics in the Environment: Current Achievements and Future Prospects, *Catalysts*, 2023, **13**, 846.
- 3 A. Galushchinskiy, R. González-Gómez, K. McCarthy, P. Farràs and A. Savateev, Progress in Development of Photocatalytic Processes for Synthesis of Fuels and Organic Compounds under Outdoor Solar Light, *Energy Fuel*, 2022, **36**, 4625–4639.
- 4 B. Ran, *et al.*, Photocatalytic Antimicrobials: Principles, Design Strategies, and Applications, *Chem. Rev.*, 2023, **123**(22), 12371–12430.
- 5 L. Buglioni, F. Raymenants, A. Slattery, S. D. A. Zondag and T. Noël, Technological Innovations in Photochemistry for Organic Synthesis: Flow Chemistry, High-Throughput Experimentation, Scale-up, and Photoelectrochemistry, *Chem. Rev.*, 2022, **122**, 2752–2906.
- 6 J. Wen, J. Xie, X. Chen and X. Li, A review on  $\text{g-C}_3\text{N}_4$ -based photocatalysts, *Appl. Surf. Sci.*, 2017, **391**, 72–123.
- 7 M. Ismael and Y. Wu, A mini-review on the synthesis and structural modification of  $\text{g-C}_3\text{N}_4$ -based materials, and their applications in solar energy conversion and environmental remediation, *Sustainable Energy Fuels*, 2019, **3**, 2907–2925.
- 8 P. Wang, Q. Zhao, W. Xiao and J. Chen, Recent advances in visible-light photoredox-catalyzed nitrogen radical cyclization, *Green Synth. Catal.*, 2020, **1**, 42–51.
- 9 P. P. Singh and V. Srivastava, Recent advances in visible-light graphitic carbon nitride ( $\text{g-C}_3\text{N}_4$ ) photocatalysts for chemical transformations, *RSC Adv.*, 2022, **12**, 18245–18265.



10 B. Tiwari and S. Ram, Biogenic Synthesis of Graphitic Carbon Nitride for Photocatalytic Degradation of Organic Dyes, *ACS Omega*, 2019, **4**, 10263–10272.

11 X. Wang, *et al.*, A metal-free polymeric photocatalyst for hydrogen production from water under visible light, *Nat. Mater.*, 2009, **8**, 76–80.

12 M. A. Qamar, *et al.*, Synthesis and applications of graphitic carbon nitride (g-C<sub>3</sub>N<sub>4</sub>) based membranes for wastewater treatment: a critical review, *Heliyon*, 2023, **9**, e12685.

13 P. Lakhani and C. K. Modi, Asymmetric Hydrogenation using Covalently Immobilized Ru-BINOL-AP@MSNs Catalyst, *New J. Chem.*, 2023, **47**, 8767–8775.

14 P. Lakhani and C. K. Modi, Spick-and-span protocol for designing of silica-supported enantioselective organocatalyst for the asymmetric aldol reaction, *Mol. Catal.*, 2022, **525**, 112359.

15 P. Lakhani, *et al.*, DFT stimulation and experimental insights of chiral Cu(ii)-salen scaffold within the pocket of MWW-zeolite and its catalytic study, *Phys. Chem. Chem. Phys.*, 2023, **25**, 14374–14386.

16 P. Lakhani, S. Kane, H. Srivastava, U. K. Goutam and C. K. Modi, Sustainable approach for the synthesis of chiral  $\beta$ -aminoketones using an encapsulated chiral Zn(ii)-salen complex, *RSC Sustainability*, 2023, **1**, 1773–1782.

17 V. Hasija, *et al.*, Advanced activation of persulfate by polymeric g-C<sub>3</sub>N<sub>4</sub> based photocatalysts for environmental remediation: a review, *J. Hazard. Mater.*, 2021, **413**, 125324.

18 A. Kumar, *et al.*, Frontier nanoarchitectonics of graphitic carbon nitride based plasmonic photocatalysts and photoelectrocatalysts for energy, environment and organic reactions, *Mater. Chem. Front.*, 2023, **7**, 1197–1247.

19 G. Q. Zhao, J. Zou, J. Hu, X. Long and F. P. Jiao, A critical review on graphitic carbon nitride (g-C<sub>3</sub>N<sub>4</sub>)-based composites for environmental remediation, *Sep. Purif. Technol.*, 2021, **279**, 119769.

20 N. Kumar, *et al.*, Graphitic carbon nitride (g-C<sub>3</sub>N<sub>4</sub>)-assisted materials for the detection and remediation of hazardous gases and VOCs, *Environ. Res.*, 2023, **231**, 116149.

21 Y. Ding, *et al.*, Emerging heterostructured C<sub>3</sub>N<sub>4</sub> photocatalysts for photocatalytic environmental pollutant elimination and sterilization, *Inorg. Chem. Front.*, 2023, **10**, 3756–3780.

22 Y. Luo, *et al.*, g-C<sub>3</sub>N<sub>4</sub>-based photocatalysts for organic pollutant removal: a critical review, *Carbon Research*, 2023, **2**(14), 1–24.

23 A. Akhundi, A. Zaker Moshfegh, A. Habibi-Yangjeh and M. Sillanpää, Simultaneous Dual-Functional Photocatalysis by g-C<sub>3</sub>N<sub>4</sub>-Based Nanostructures, *ACS ES&T Engg.*, 2022, **2**, 564–585.

24 X. L. Song, L. Chen, L. J. Gao, J. T. Ren and Z. Y. Yuan, Engineering g-C<sub>3</sub>N<sub>4</sub> based materials for advanced photocatalysis: recent advances, *Green Energy Environ.*, 2022, DOI: [10.1016/j.gee.2022.12.005](https://doi.org/10.1016/j.gee.2022.12.005).

25 A. Alaghmandfar and K. Ghandi, A Comprehensive Review of Graphitic Carbon Nitride (g-C<sub>3</sub>N<sub>4</sub>)-Metal Oxide-Based Nanocomposites: Potential for Photocatalysis and Sensing, *Nanomaterials*, 2022, **12**, 294.

26 F. K. Butt, S. Ullah, J. Ahmad, S. U. Rehman and Z. Tariq, Graphitic Carbon Nitride/Metal Oxides Nanocomposites and Their Applications in Engineering, *Compos. Mater. Appl. Eng. Biomed. Food Sci.*, 2020, pp. 231–265.

27 X. Liu, *et al.*, Recent developments of doped g-C<sub>3</sub>N<sub>4</sub> photocatalysts for the degradation of organic pollutants, *Crit. Rev. Environ. Sci. Technol.*, 2021, **51**, 751–790.

28 P. Lakhani and C. K. Modi, Shaping enantiochemistry: recent advances in enantioselective reactions via heterogeneous chiral catalysis, *Mol. Catal.*, 2023, **548**, 113429.

29 X. Yang, L. Zhao, S. Wang, J. Li and B. Chi, Recent progress of g-C<sub>3</sub>N<sub>4</sub> applied in solar cells, *J. Mater.*, 2021, **7**, 728–741.

30 Y. Chen and X. Bai, A review on quantum dots modified g-C<sub>3</sub>N<sub>4</sub>-based photocatalysts with improved photocatalytic activity, *Catalysts*, 2020, **10**, 142.

31 N. S. N. Hasnan, M. A. Mohamed and Z. A. Mohd Hir, Surface Physicochemistry Modification and Structural Nanoarchitectures of g-C<sub>3</sub>N<sub>4</sub> for Wastewater Remediation and Solar Fuel Generation, *Adv. Mater. Technol.*, 2022, **7**, 2100993.

32 S. Dolai, S. K. Bhunia, P. Kluson, P. Stavarek and A. Pittermannova, Solvent-Assisted Synthesis of Supramolecular-Assembled Graphitic Carbon Nitride for Visible Light Induced Hydrogen Evolution – A Review, *ChemCatChem*, 2022, **14**, e202101299.

33 J. Wang and S. Wang, A critical review on graphitic carbon nitride (g-C<sub>3</sub>N<sub>4</sub>)-based materials: preparation, modification and environmental application, *Coord. Chem. Rev.*, 2022, **453**, 214338.

34 A. Dandia, *et al.*, Structure couture and appraisal of catalytic activity of carbon nitride (g-C<sub>3</sub>N<sub>4</sub>) based materials towards sustainability, *Curr. Res. Green Sustainable Chem.*, 2020, **3**, 100039.

35 V. Srivastava, P. K. Singh and P. P. Singh, Recent advances of visible-light photocatalysis in the functionalization of organic compounds, *J. Photochem. Photobiol. C*, 2022, **50**, 100488.

36 S. Kumar, S. Karthikeyan and A. F. Lee, g-C<sub>3</sub>N<sub>4</sub>-based nanomaterials for visible light-driven photocatalysis, *Catalysts*, 2018, **8**, 74.

37 A. Thomas, *et al.*, Graphitic carbon nitride materials: variation of structure and morphology and their use as metal-free catalysts, *J. Mater. Chem.*, 2008, **18**, 4893–4908.

38 J. Liu, *et al.*, Metal-free efficient photocatalyst forstable visible water splitting via atwo-electron pathway, *Science*, 2015, **347**, 970–974.

39 K. Maślana, R. J. Kaleńczuk, B. Zielińska and E. Mijowska, Synthesis and characterization of nitrogen-doped carbon nanotubes derived from g-C<sub>3</sub>N<sub>4</sub>, *Materials*, 2020, **13**, 1349.

40 L. Wang, *et al.*, Graphitic carbon nitride-based photocatalytic materials: preparation strategy and application, *ACS Sustain. Chem. Eng.*, 2020, **8**, 16048–16085.



41 A. Hayat, *et al.*, State of the art advancement in rational design of g-C<sub>3</sub>N<sub>4</sub> photocatalyst for efficient solar fuel transformation, environmental decontamination and future perspectives, *Int. J. Hydrogen Energy*, 2022, **47**, 10837–10867.

42 C. K. Bandoh, E. S. Agorku and F. K. Ampong, Graphitic Carbon Nitride Based Composites as Advanced Photocatalysts, from Synthesis to Application: A Review, *Res. Rev.: J. Mater. Sci.*, 2022, **10**, 1–17.

43 W. Iqbal, *et al.*, Controllable synthesis of graphitic carbon nitride nanomaterials for solar energy conversion and environmental remediation: the road travelled and the way forward, *Catal. Sci. Technol.*, 2018, **8**, 4576–4599.

44 H. Ghafuri, Z. Tajik, N. Ghanbari and P. Hanifehnejad, Preparation and characterization of graphitic carbon nitride-supported l-arginine as a highly efficient and recyclable catalyst for the one-pot synthesis of condensation reactions, *Sci. Rep.*, 2021, **11**, 19792.

45 L. Wang, C. Wang, X. Hu, H. Xue and H. Pang, Metal/Graphitic Carbon Nitride Composites: Synthesis, Structures, and Applications, *Chem.-Asian J.*, 2016, **11**, 3305–3328.

46 W. Shang, *et al.*, Synergistic Redox Reaction for Value-Added Organic Transformation via Dual-Functional Photocatalytic Systems, *ACS Catal.*, 2021, **11**, 4613–4632.

47 J. Vasiljević, I. Jerman and B. Simončič, Graphitic carbon nitride as a new sustainable photocatalyst for textile functionalization, *Polymers*, 2021, **13**, 2568.

48 A. Behera, A. K. Kar and R. Srivastava, Challenges and prospects in the selective photoreduction of CO<sub>2</sub>to C<sub>1</sub> and C<sub>2</sub> products with nanostructured materials: a review, *Mater. Horiz.*, 2022, **9**, 607–639.

49 M. Ismael, Hydrogen production via water splitting over graphitic carbon nitride (g-C<sub>3</sub>N<sub>4</sub>)-based photocatalysis, *Process Syst. Eng. a Smooth Energy Transit.*, 2022, **8**, pp. 1–39.

50 J. C. Wang, *et al.*, Mn-Doped g-C<sub>3</sub>N<sub>4</sub> Nanoribbon for Efficient Visible-Light Photocatalytic Water Splitting Coupling with Methylene Blue Degradation, *ACS Sustain. Chem. Eng.*, 2018, **6**, 8754–8761.

51 Y. Che, *et al.*, Plasmonic ternary hybrid photocatalyst based on polymeric g-C<sub>3</sub>N<sub>4</sub> towards visible light hydrogen generation, *Sci. Rep.*, 2020, **10**, 721.

52 S. Qin, *et al.*, Real-Time Adsorption and Photodegradation Investigation of Dye Removal on g-C<sub>3</sub>N<sub>4</sub> Surface by Attenuated Total Reflectance Induced Evanescent Spectroscopy, *J. Phys. Chem. C*, 2021, **125**, 4027–4040.

53 A. Modwi, A. Albadri and K. K. Taha, High Malachite Green Dye Removal by ZrO<sub>2</sub>-g-C<sub>3</sub>N<sub>4</sub> (ZOCN) Meso-sorbent: Characteristics and Adsorption Mechanism, *Diamond Relat. Mater.*, 2023, **132**, 109698.

54 H. B. Fang, Y. Luo, Y. Z. Zheng, W. Ma and X. Tao, Facile Large-Scale Synthesis of Urea-Derived Porous Graphitic Carbon Nitride with Extraordinary Visible-Light Spectrum Photodegradation, *Ind. Eng. Chem. Res.*, 2016, **55**, 4506–4514.

55 A. Kharlamov, M. Bondarenko, G. Kharlamova and N. Gubareni, Features of the synthesis of carbon nitride oxide (g-C<sub>3</sub>N<sub>4</sub>)O at urea pyrolysis, *Diamond Relat. Mater.*, 2016, **66**, 16–22.

56 A. Hayat, *et al.*, Graphitic carbon nitride (g-C<sub>3</sub>N<sub>4</sub>)-based semiconductor as a beneficial candidate in photocatalysis diversity, *Int. J. Hydrogen Energy*, 2022, **47**, 5142–5191.

57 B. Yuan, *et al.*, Physical vapor deposition of graphitic carbon nitride (g-C<sub>3</sub>N<sub>4</sub>) films on biomass substrate: optoelectronic performance evaluation and life cycle assessment, *Adv. Compos. Hybrid Mater.*, 2022, **5**, 813–822.

58 M. I. Chebanenko, *et al.*, Chemical and structural changes of g-C<sub>3</sub>N<sub>4</sub> through oxidative physical vapor deposition, *Appl. Surf. Sci.*, 2022, **600**, 154079.

59 E. B. Chubenko, N. G. Kovalchuk, I. V. Komissarov and V. E. Borisenko, Chemical Vapor Deposition of 2D Crystallized g-C<sub>3</sub>N<sub>4</sub> Layered Films, *J. Phys. Chem. C*, 2022, **126**, 4710–4714.

60 R. M. Yadav, *et al.*, Facile synthesis of highly fluorescent free-standing films comprising graphitic carbon nitride (g-C<sub>3</sub>N<sub>4</sub>) nanolayers, *New J. Chem.*, 2020, **44**, 2644–2651.

61 A. Raza, H. Shen, A. A. Haidry and S. Cui, Hydrothermal synthesis of Fe<sub>3</sub>O<sub>4</sub>/TiO<sub>2</sub>/g-C<sub>3</sub>N<sub>4</sub>: advanced photocatalytic application, *Appl. Surf. Sci.*, 2019, **488**, 887–895.

62 A. R. Kuldeep, R. S. Dhabbe and K. M. Garadkar, Development of g-C<sub>3</sub>N<sub>4</sub>-TiO<sub>2</sub> visible active hybrid photocatalyst for the photodegradation of methyl orange, *Res. Chem. Intermed.*, 2021, **47**, 5155–5174.

63 F. Idrees, R. Dillert, D. Bahnemann, F. K. Butt and M. Tahir, In-situ synthesis of Nb<sub>2</sub>O<sub>5</sub>/g-C<sub>3</sub>N<sub>4</sub> heterostructures as highly efficient photocatalysts for molecular h<sub>2</sub> evolution under solar illumination, *Catalysts*, 2019, **9**, 169.

64 L. Kunhikrishnan, K. Vishal and S. Palaniyappan, Mechanical and Thermal Characterization on Synthesized Silane-Treated Graphitic Carbon Nitride (g-C<sub>3</sub>N<sub>4</sub>) Reinforced 3D Printed Poly (Lactic Acid) Composite, *J. Inorg. Organomet. Polym. Mater.*, 2023, **33**, 1234–1245.

65 S. Wu, *et al.*, A simple synthesis route of sodium-doped g-C<sub>3</sub>N<sub>4</sub> nanotubes with enhanced photocatalytic performance, *J. Photochem. Photobiol. A*, 2021, **406**, 112999.

66 J. Xi, *et al.*, Preparation of high porosity biochar materials by template method: a review, *Environ. Sci. Pollut. Res.*, 2020, **27**, 20675–20684.

67 K. Li, *et al.*, Template-Assisted Surface Hydrophilicity of Graphitic Carbon Nitride for Enhanced Photocatalytic H<sub>2</sub>Evolution, *ACS Appl. Energy Mater.*, 2021, **4**, 12965–12973.

68 F. T. Li, *et al.*, Precipitation synthesis of mesoporous photoactive Al<sub>2</sub>O<sub>3</sub> for constructing g-C<sub>3</sub>N<sub>4</sub>-based heterojunctions with enhanced photocatalytic activity, *Ind. Eng. Chem. Res.*, 2014, **53**, 19540–19549.

69 M. Hao, *et al.*, In-situ hard template synthesis of mesoporous carbon/graphite carbon nitride (C/CN-T-x) composites with high photocatalytic activities under visible light irradiation, *Solid State Sci.*, 2020, **109**, 106428.

70 J. Liu, *et al.*, Controlled synthesis of ordered mesoporous g-C<sub>3</sub>N<sub>4</sub> with a confined space effect on its photocatalytic activity, *Mater. Sci. Semicond. Process.*, 2016, **46**, 59–68.



71 C. T. Yang, *et al.*, A novel heterojunction photocatalyst, Bi<sub>2</sub>SiO<sub>5</sub>/g-C<sub>3</sub>N<sub>4</sub>: synthesis, characterization, photocatalytic activity, and mechanism, *RSC Adv.*, 2016, **6**, 40664–40675.

72 T. S. Bui, P. Bansal, B. K. Lee, T. Mahvelati-Shamsabadi and T. Soltani, Facile fabrication of novel Ba-doped g-C<sub>3</sub>N<sub>4</sub> photocatalyst with remarkably enhanced photocatalytic activity towards tetracycline elimination under visible-light irradiation, *Appl. Surf. Sci.*, 2020, **506**, 144184.

73 H. Starukh and P. Praus, Doping of graphitic carbon nitride with non-metal elements and its applications in photocatalysis, *Catalysts*, 2020, **10**, 1–38.

74 M. A. Qamar, M. Javed, S. Shahid and M. Sher, Fabrication of g-C<sub>3</sub>N<sub>4</sub>/transition metal (Fe, Co, Ni, Mn and Cr)-doped ZnO ternary composites: excellent visible light active photocatalysts for the degradation of organic pollutants from wastewater, *Mater. Res. Bull.*, 2022, **147**, 111630.

75 H. Jiang, Y. Li, D. Wang, X. Hong and B. Liang, Recent Advances in Heteroatom Doped Graphitic Carbon Nitride (g-C<sub>3</sub>N<sub>4</sub>) and g-C<sub>3</sub>N<sub>4</sub>/Metal Oxide Composite Photocatalysts, *Curr. Org. Chem.*, 2020, **24**, 673–693.

76 L. Tan, *et al.*, Novel two-dimensional crystalline carbon nitrides beyond g-C<sub>3</sub>N<sub>4</sub>: structure and applications, *J. Mater. Chem. A*, 2021, **9**, 17–33.

77 Y. Rangraz, M. M. Heravi and A. Elhampour, Recent Advances on Heteroatom-Doped Porous Carbon/Metal Materials: Fascinating Heterogeneous Catalysts for Organic Transformations, *Chem. Rec.*, 2021, **21**, 1985–2073.

78 P. P. Singh, Nitride (g-C<sub>3</sub>N<sub>4</sub>) photocatalysts for chemical transformations, *RSC Adv.*, 2022, **12**, 18245–18265.

79 P. K. Singh, S. R. Bhardiya, A. Asati, V. K. Rai and M. Singh, Cu/Cu<sub>2</sub>O@g-C<sub>3</sub>N<sub>4</sub>: Recyclable Photocatalyst under Visible Light to Access 2-Aryl/benzimidazoles/benzothiazoles in Water, *ChemistrySelect*, 2020, **5**, 14270–14275.

80 Y. Wu, Y. Wang and M. Li, Progress in Photocatalysis of g-C<sub>3</sub>N<sub>4</sub> and its Modified Compounds, *E3S Web Conf.*, 2021, **114**, 1–6.

81 J. Xiao, *et al.*, Heterogeneous Photocatalytic Organic Transformation Reactions Using Conjugated Polymers-Based Materials, *ACS Catal.*, 2020, **10**, 12256–12283.

82 N. Rajalakshmi, D. Barathi, S. Meyvel and P. Sathya, S-scheme Ag<sub>2</sub>CrO<sub>4</sub>/g-C<sub>3</sub>N<sub>4</sub> photocatalyst for effective degradation of organic pollutants under visible light, *Inorg. Chem. Commun.*, 2021, **132**, 10849.

83 D. Bhandari, P. Lakhani, A. Sharma, S. Soni and C. K. Modi, Efficient Visible Light Active Photocatalyst: Magnesium Oxide Doped Graphitic Carbon Nitride for Knoevenagel Condensation Reaction, *ACS Appl. Eng. Mater.*, 2023, **10**, 2752–2764.

84 B. A. Maru, *et al.*, Fe@g-C<sub>3</sub>N<sub>4</sub>: an effective photocatalyst for Baeyer–Villiger oxidation under visible light condition, *New J. Chem.*, 2023, **47**, 9797–9805.

85 I. Camussi, *et al.*, G-C<sub>3</sub>N<sub>4</sub> - Singlet Oxygen Made Easy for Organic Synthesis: Scope and Limitations, *ACS Sustain. Chem. Eng.*, 2019, **7**, 8176–8182.

86 S. Sharma, R. Nazir, S. Pande and B. R. Sarkar, Microwave-Assisted Efficient Suzuki-Miyaura Cross-Coupling Reactions in Water Catalyzed by Nano-Pd/g-C<sub>3</sub>N<sub>4</sub> Composite, *ChemistrySelect*, 2017, **2**, 8745–8750.

87 F. Verma, *et al.*, Visible light-induced direct conversion of aldehydes into nitriles in aqueous medium using Co@g-C<sub>3</sub>N<sub>4</sub> as photocatalyst, *Catal. Commun.*, 2019, **119**, 76–81.

88 H. Gao, *et al.*, Synthesis of 3-Arylquinoxalin-2(1H)-ones under Visible-Light Irradiation with Oxygen-Doped Carbon Nitride as Heterogenous Photocatalyst, *Eur. J. Org. Chem.*, 2023, **26**, e202300252.

89 S. Zhao, *et al.*, Ag<sub>2</sub>CO<sub>3</sub>-derived Ag/g-C<sub>3</sub>N<sub>4</sub> composite with enhanced visible-light photocatalytic activity for hydrogen production from water splitting, *Int. J. Hydrogen Energy*, 2020, **45**, 20851–20858.

90 J. E. Samaniego-Benitez, K. Jimenez-Rangel, L. Lartundo-Rojas, A. García-García and A. Mantilla, Enhanced photocatalytic H<sub>2</sub> production over g-C<sub>3</sub>N<sub>4</sub>/NiS hybrid photocatalyst, *Mater. Lett.*, 2021, **290**, 129476.

91 W. Li, *et al.*, Hydrogen evolution by catalyzing water splitting on two-dimensional g-C<sub>3</sub>N<sub>4</sub>-Ag/AgBr heterostructure, *Appl. Surf. Sci.*, 2019, **494**, 275–284.

92 Y. Li, *et al.*, Journal of Colloid and Interface Science In situ Synthesis of a Novel Mn<sub>3</sub>O<sub>4</sub>/g-C<sub>3</sub>N<sub>4</sub> p–n Heterostructure Photocatalyst for Water Splitting, *J. Colloid Interface Sci.*, 2020, **586**, 778–784.

93 W. S. Chai, *et al.*, A review on conventional and novel materials towards heavy metal adsorption in wastewater treatment application, *J. Cleaner Prod.*, 2021, **296**, 126589.

94 Y. Shi, *et al.*, Evaluation of self-cleaning performance of the modified g-C<sub>3</sub>N<sub>4</sub> and GO based PVDF membrane toward oil-in-water separation under visible-light, *Chemosphere*, 2019, **230**, 40–50.

95 R. Manimozhi, M. Mathankumar and A. P. G. Prakash, Synthesis of g-C<sub>3</sub>N<sub>4</sub>/ZnO heterostructure photocatalyst for enhanced visible degradation of organic dye, *Optik*, 2021, **229**, 165548.

96 S. Kumaravel, M. Manoharan and Y. Haldorai, Enhanced visible-light degradation of organic dyes via porous g-C<sub>3</sub>N<sub>4</sub>, *Phosphorus, Sulfur Silicon Relat. Elem.*, 2022, **197**, 200–208.

97 Y. Zou, *et al.*, SnO<sub>2</sub> quantum dots anchored on g-C<sub>3</sub>N<sub>4</sub> for enhanced visible-light photocatalytic removal of NO and toxic NO<sub>2</sub> inhibition, *Appl. Surf. Sci.*, 2019, **496**, 143630.

98 I. Papailias, *et al.*, Selective removal of organic and inorganic air pollutants by adjusting the g-C<sub>3</sub>N<sub>4</sub>/TiO<sub>2</sub> ratio, *Catal. Today*, 2021, **361**, 37–42.

99 Y. Huang, *et al.*, g-C<sub>3</sub>N<sub>4</sub>/TiO<sub>2</sub> Composite Film in the Fabrication of a Photocatalytic Air-Purifying Pavements, *Sol. RRL*, 2020, **4**, 2000170.

100 M.-T. Pham, D. P. H. Tran, X.-T. Bui and S.-J. You, Rapid Fabrication of MgO@g-C<sub>3</sub>N<sub>4</sub> Heterojunction for Photocatalytic Nitric Oxide degradation under Visible Light, *Beilstein Arch.*, 2022, **30**, 1141–1154.

101 J. He, P. Lv, J. Zhu and H. Li, Selective CO<sub>2</sub> reduction to HCOOH on a Pt/In<sub>2</sub>O<sub>3</sub>/g-C<sub>3</sub>N<sub>4</sub> multifunctional visible-light photocatalyst, *RSC Adv.*, 2020, **10**, 22460–22467.



102 X. X. Jiang, *et al.*, Tailoring the properties of g-C<sub>3</sub>N<sub>4</sub> with CuO for enhanced photoelectrocatalytic CO<sub>2</sub> reduction to methanol, *J. CO<sub>2</sub> Util.*, 2020, **40**, 101222.

103 W. Yu, D. Xu and T. Peng, Enhanced photocatalytic activity of g-C<sub>3</sub>N<sub>4</sub> for selective CO<sub>2</sub> reduction to CH<sub>3</sub>OH via facile coupling of ZnO: a direct Z-scheme mechanism, *J. Mater. Chem. A*, 2015, **3**, 19936–19947.

104 S. Singh, A. Modak and K. Kishore, CO<sub>2</sub> Reduction to Methanol Using a Conjugated Organic – Inorganic Hybrid - TiO<sub>2</sub> – C<sub>3</sub>N<sub>4</sub> Nano - assembly, *Transactions of the Indian National Academy of Engineering*, 2021, **6**, 395–404.

105 K. Rabé, L. Liu, N. A. Nahyoon, Y. Zhang and A. M. Idris, Visible-light photocatalytic fuel cell with Z-scheme g-C<sub>3</sub>N<sub>4</sub>/FeO/TiO<sub>2</sub> anode and WO<sub>3</sub> cathode efficiently degrades berberine chloride and stably generates electricity, *Sep. Purif. Technol.*, 2019, **212**, 774–782.

106 K. Rabé, L. Liu and N. A. Nahyoon, Electricity generation in fuel cell with light and without light and decomposition of tetracycline hydrochloride using g-C<sub>3</sub>N<sub>4</sub>/FeO(1%)/TiO<sub>2</sub> anode and WO<sub>3</sub> cathode, *Chemosphere*, 2020, **243**, 125425.

107 Z. L. Yang, *et al.*, High-performance g-C<sub>3</sub>N<sub>4</sub> added carbon-based perovskite solar cells insulated by Al<sub>2</sub>O<sub>3</sub> layer, *Sol. Energy*, 2019, **193**, 859–865.

108 J. Yang, Y. Ma, J. Yang, W. Liu and X. Li, Recent Advances in g-C<sub>3</sub>N<sub>4</sub> for the Application of Perovskite Solar Cells, *Nanomaterials*, 2022, **12**, 1–14.

109 H. Yu, *et al.*, Novel application of a Z-scheme photocatalyst of Ag<sub>3</sub>PO<sub>4</sub>@g-C<sub>3</sub>N<sub>4</sub> for photocatalytic fuel cells, *J. Environ. Manage.*, 2020, **254**, 109738.

